OPTICAL RESPONSE OF THE ATMOSPHERE DURING THE CARIBBEAN TOTAL SOLAR ECLIPSES OF 26 FEBRUARY 1998 AND OF 3 FEBRUARY 1916 AT FALCÓN STATE, VENEZUELA

MARCOS A. PEÑALOZA-MURILLO*
University of Essex, Environmental Research Laboratory, Central Campus. Wivenhoe Park, Colchester, Essex CO4 3SQ, UK and Universidad de Los Andes, Facultad de Ciencias, Equipo Interdisciplinario e Interdepartamental de Investigación Atmosférica Mérida, Edo. Mérida. Venezuela

(Received 31 January 2002; Accepted 10 September 2002)

Abstract. An investigation of the optical response of the atmosphere before, during, and after the total solar eclipse of 26 February 1998 at the Caribbean Peninsula of Paraguaná (Falcón State) in Venezuela, was made by measuring photometrically the intensity of the sky brightness in three strategic directions: zenith, horizon anti-parallel or opposite the umbra path, and horizon perpendicular to this path. From these measurements, and by applying in an inverse way an empirical photometric model, very rough estimations of the extinction coefficient, and also of the average optical depth, were obtained in one of these particular directions. However based on meteorological measurements such as those of relative humidity and temperature, and applying a different model, a better estimation in the visual of the total global extinction coefficient of the sky (except the horizon), were made considering the contribution of each component: atmospheric aerosol, water vapour, ozone and Rayleigh scattering. It is shown that this global coefficient is mostly dependent upon aerosol extinction. In spite of the strong reduction of sky brightness photometrically observed during the totality, the results show that the sky was not dark. This is confirmed by the results obtained for the total global extinction coefficient. Additionally it is estimated that the total solar eclipse that took place also in Falcón State, Venezuela, at the beginning of the last century on 3 February 1916, was ∼30% darker that the 1998 eclipse, and that atmospheric aerosol played a relevant and similar role in the scattering of sunlight during the totality as it was for 1998's. Visual observations made during each event, which show that at length only one or two bright stars could be seen in the sky, support the results obtained for both eclipses.

Keywords: Atmospheric aerosol influence, meteorological measurements, photometric measurements, sky brightness, solar eclipse, tropic

1. Introduction

On Thursday 26th February 1998 the last total solar eclipse for Latin America of the past century and millennium, and the eclipse No. 51 (out of 73) in the Saros Series 130 of solar eclipses, took place. In particular it was seen from northern South America, some Caribbean islands (Kuiper and van der Woude, 1998), and some Pacific islands near the Latin-American west coast (for a general description

* Permanent affiliation: E-mail: mpenaloa@ula.ve

Earth, Moon and Planets **91:** 125–159, 2002.

and coverage, see *New Scientist*, April 1998, *Sky & Telescope*, May 1998, and *Journal of the British Astronomical Association*, June 1998). Venezuela was one of three continental countries where this eclipse could be observed (Figure 1) and, in fact, it was the fourth time during that century that the Moon shadow cone swept or touched Venezuelan territory. The first one was on 3 February 1916, the second one was on 1 October 1940 (USNO, 1939), and the third one on 12 October 1977 (Fiala, 1976). These last two, unfortunately, either passed over a very remote region in the jungle (southern Amazonas state) which at that time was almost uninhabited and hard to reach, or occurred when the eclipsed Sun was already at the sunset (at Puerto Ayacucho, Amazonas State capital), respectively. Neglecting these two, the first one and the most recent one have been the total solar eclipses that have draw the attention of Venezuelan people, mainly, because one was at the end of the morning (1916) and the other during the first half of the afternoon (1998) both covering well-populated regions of the country (Ugueto, 1916; Espenak and Anderson, 1996). Ugueto (1916) and del Castillo et al. (1916) published reports in which they account for some astronomical, atmospheric and meteorological observations for the eclipse of 1916. Other reports, such as those by Sifontes (1920), Röhl (1932) and Peñaloza (1975), however, account only for meteorological or astronomical observations in three of the solar partial eclipses which took place in Venezuela in the twentieth century many times. Thus eighty-two years had to elapse from 1916 until a new opportunity arrived for observing a total eclipse of the Sun from Venezuela. The present research focused on carrying out photometric observations of the visual sky brightness at the zenith and on the horizon during the total solar eclipse on 26 February 1998 at the Caribbean Peninsula of Paraguaná (Figure 2). This is located in the northern part of the north-west Venezuelan State of Falcón.

Ignoring the light of the solar corona and air-glow, the visual sky brightness during a total solar eclipse is produced in part by atmospheric aerosol particles which at least scatter light taking place within the penumbra (first order scattering) and scatter light taking place within the umbra (second order scattering) as a consequence of a first order scattering within the penumbra, as depicted in Figure 3 (Zirker, 1995). Therefore the ambient or environmental conditions of the air of a particular area or region determine the local conditions by which the visual sky brightness is produced and thereby observed during a total solar eclipse. The sky could be darker or brighter depending on the air quality during the totality around the observation zone. It is interesting to note that reports of darkness during total solar eclipses in the ninetieth century indicate that they were darker than those of the twentieth century (Silverman and Mullen, 1974). This is, of course, circumstantial since it depends on the local air quality of the observation site which, in turn, depends on the variability of atmospheric pollution. Today pollution is stronger and potentially can contribute to make less dark the sky during a total solar eclipse when it is being observed from urban or industrial areas.

It is interesting to highlight that before 1944 it was believed that the general brightness of the sky during the full phase of a total solar eclipse was due to the

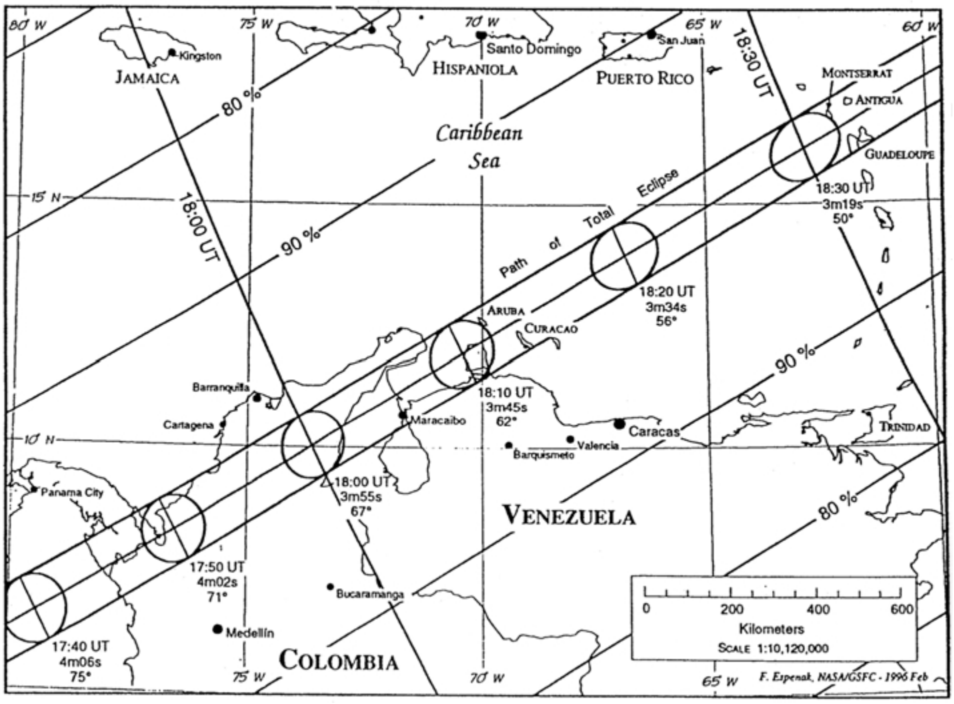

Figure 1. The eclipse path through northern South America and the Caribbean. The shadow passed over Maracaibo city, the biggest one along the path and the second biggest one of Venezuela (Espenak and Anderson, 1996).

brightness of the solar corona. It was not until Betenska (1944) definitely confirmed that the part played by the light of the solar corona in the general brightness of the sky and the illumination of the landscape is insignificant and that this brightness is related to the light coming from the surrounding atmosphere and which penetrates into the shadow. However an early account given by Lockyer (1927) on the total solar of eclipse of 29 June 1927 in England (Marriot, 1999) showed that the light emitted by the corona was evidently not very great because this observer could not record any perceptible shadow being cast by it on a white sheet, in spite of the fact that the corona was exceedingly bright (on this point, see *The Illumination Engineer*, July 1928, p. 128). This lead to the idea that the illumination during totality is due mainly to diffused daylight by the atmosphere.

Although the sky brightness is dependent not only on the particular direction of sight but also on the solar elevation during a solar eclipse (Schaefer, 1993), as on a normal day, the photometric observations were made in the zenith and in the horizon. The closer toward the zenith is looked at, the larger is the proportion of multiply-scattered light observed. Looking towards the horizon the scattered light will include a proportion that is singly scattered. The zenith has been the sky point most photometrically observed during the occurrence of a total solar

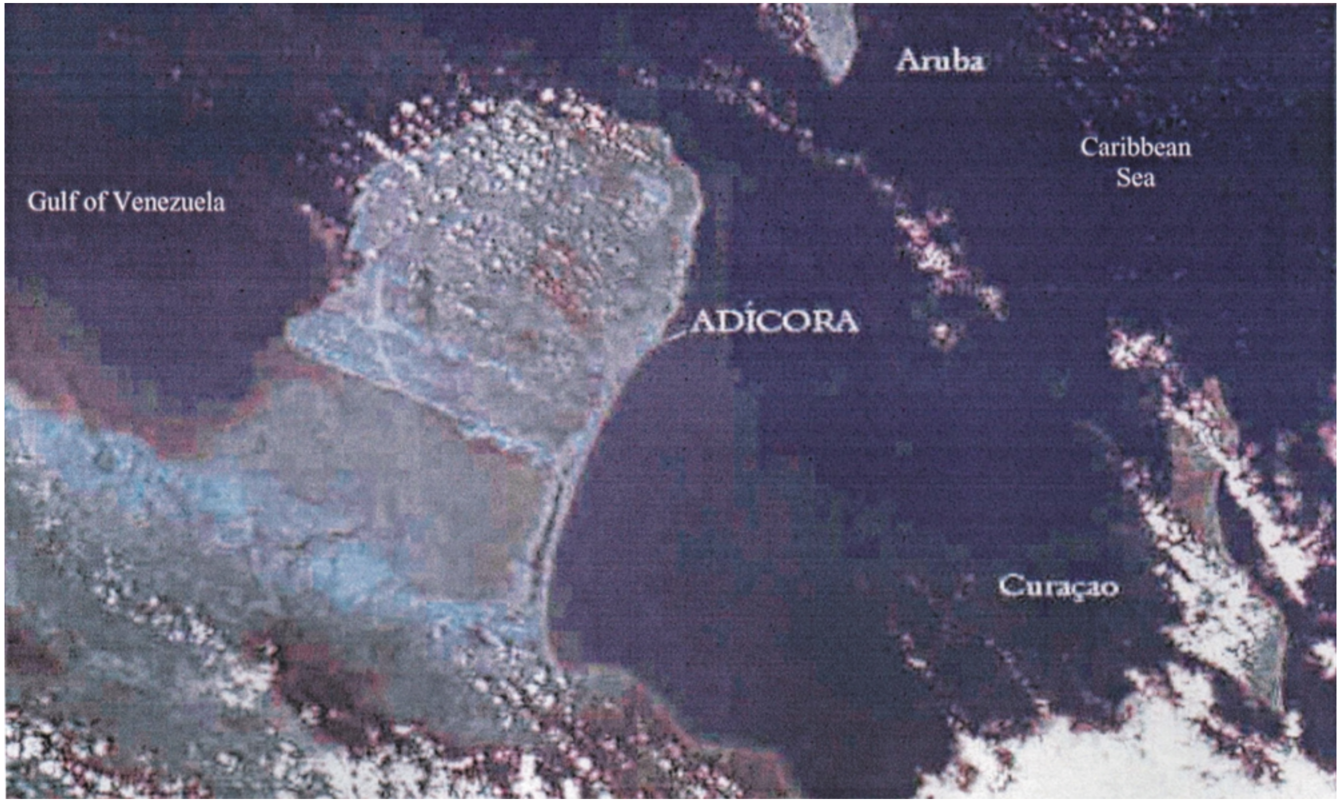

Figure 2. Clear picture of the head-shaped Peninsula of Paraguaná from space taken by the KIDSAT camera on board the space shuttle. This peninsula is a semi-arid zone connected to mainland through a very narrow strip of land called the Isthmus of the Medanos (seen in the picture like a "neck"). The Gulf of Venezuela is to the left (photo courtesy of NASA).

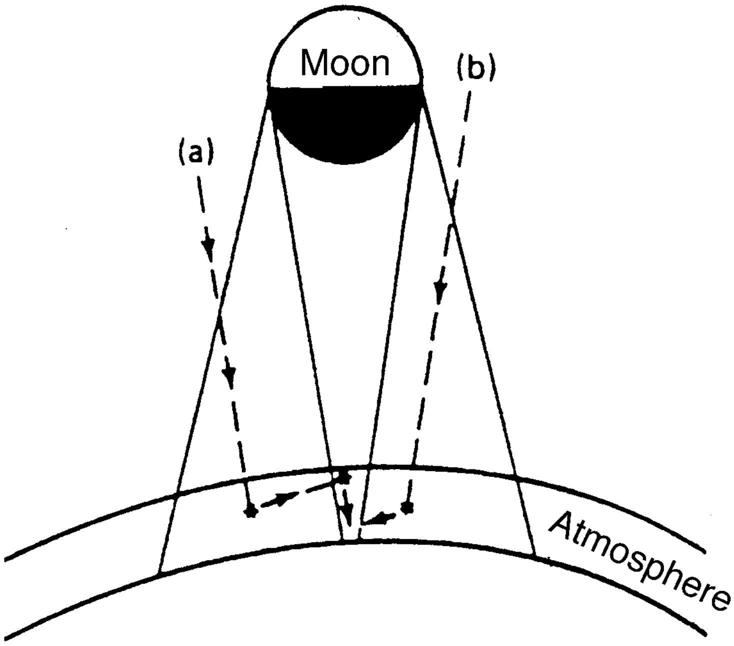

Figure 3. During a total solar eclipse multiple scattering in the Earth's atmosphere can take place. An instrument in the umbral shadow measuring towards the zenith receives sunlight that has been scattered twice as in (a); towards the horizon, the instrument measures sunlight scattered once as in (b) (adapted from Zirker, 1995).

eclipse (Silverman and Mullen, 1974). Since Halley (1715) made the first report of his solar eclipse visual observations, it also has been thoroughly reported by an appreciable number of observers that it is on the horizon that major dramatic changes in brightness and colour take place during a total solar eclipse.

The photometric results presented in the first part of this paper are observational and no theoretical evaluation is made. Potential theoretical interpretation of them (or of future eclipses) could be attempted considering the approximate models published by Gedzelman (1975), and Shaw (1978), respectively. Unfortunately the equipment used in this work did not allow for measurements depending on a specific wavelength. In addition it is necessary to take into account the particular characteristics of each eclipse observation site (surface albedo, geometrical and terrain factors, environmental measurements related to atmospheric aerosol characterisation, etc.), and also the characteristic of the measurements made (wavelength, instrumentation, region of the sky measured, etc.).

By applying, empirical models given by Schaefer (1993), results derived from these photometric measurements and those made by others of meteorological parameters, such as relative humidity and temperature, during the whole eclipse, are presented for the extinction coefficient. Based on these results an estimation of the sky darkness or brightness degree during the totality of the 1998 eclipse is made for the observation site considering the contribution of each atmospheric component, namely, atmospheric aerosol, water vapour, ozone, and Rayleigh scattering. Using the meteorological data published by Ugueto (1916) for the 1916 total solar eclipse, additional results were obtained and a comparison between these two eclipses could be made. The paper closes with a summary of the results obtained and conclusions.

2. Local Circumstances of the Eclipse Observation Site

For Venezuela the eclipse covered the north–western part of the country, including Maracaibo, the second biggest Venezuelan city. Then, the Moon shadow swept, in a south–west to north–east direction, the Gulf of Venezuela passing next over the Paraguaná Peninsula (Espenak and Anderson, 1996) where the observation site for this project was chosen. In particular, this site was located in a semi-remote and semi-arid flat area in the northern part of the Peninsula called Punta de Barco, at 69°55′54″ W, 12°09′52.8″ N, and 0 m above sea level, as reported by ARVAL amateur team (from Caracas, and hereafter referred to simply as the Arval Observatory), where the central line of the totality crossed through (Figure 4). The former installations of the booster station of "La Voz de Venezuela" Radio at this place, near the beach, served as a camp and to set up the equipment. For this place the eclipse astronomical circumstances were: first contact at 12:38:20, second contact at 14:09:18, midtotality at 14:11:10, third contact at 14:13:02, fourth contact at 15:35:43, all these times are given in local time (UT-4). The Sun altitudes were 69° for the 1st contact, 62° for the mideclipse, and 45° for the 4th contact. The totality lasted 3 min 44 s (Arval Observatory). To the unaided eye the atmospheric conditions for the day of the eclipse were in general good and acceptable. However some cloudiness near the horizon was reported by the ARVAL Observatory around the observation site being the maximum of 5/8 at 10:30 am and the minimum of 1/8 between 12:30 pm and 5:00 pm. A variation of approximately −5 °C in temperature was noted between 12:42 and 14:12 (local time) due to the eclipse. Figure 5 displays a sequence of six satellite images taken on 26th February 1998 of western Venezuela by the NASA satellite GOES-10, including Paraguaná Peninsula, showing the cloudiness variation at different times over this region. Note that at 11:08:00 am, local time, there were some clouds around the zenith of the observation site (Figure 5a). Later on the 1/8 cloudiness referred to above was located to the north of the Peninsula over the sea (Figures 5b–f), and the zone remained practically with clear sky. In particular Figure 5c shows the shadow falling to the west before crossing the peninsular area (at 01:44:00 pm local time), and Figure 5d shows the shadow crossing it (at 02:08:00 pm local time). The penumbra is also seen in these pictures. Anderson (1999) analysing two of the GOES images, describes the general pattern cloudiness and its processes originated in this region, as well as in the northern part of the country, due to this crossing.

Figure 4. Map of the Paraguaná Peninsula showing the central line of the shadow (green line) crossing it. This line entered at Punta Jacuque and left the Peninsula at Punta de Barco (just in the top to the right) where the observations were made (map courtesy of ARVAL Observatory).

3. Instrumentation and Experimental Procedure

The photometric measurements were made by means of three different photosensors: one photosensor was a Macam detector, model SD10Q-Cos (No. 1738), 15 mm^2 area, hemispherical field-of-view (∼180°), covering wavelengths from 400 nm to 700 nm and with a maximum spectral response at 560 nm; the second was an RS (stock no. 308-067), 5 mm^2 area, 17.1° field-of-view, covering wavelengths from 300–1200 nm, and a maximum spectral response at 900 nm; and a third one was an Ealing Electro-Optics (EEO) Broad Band Silicon Detector, 0.38 cm^2

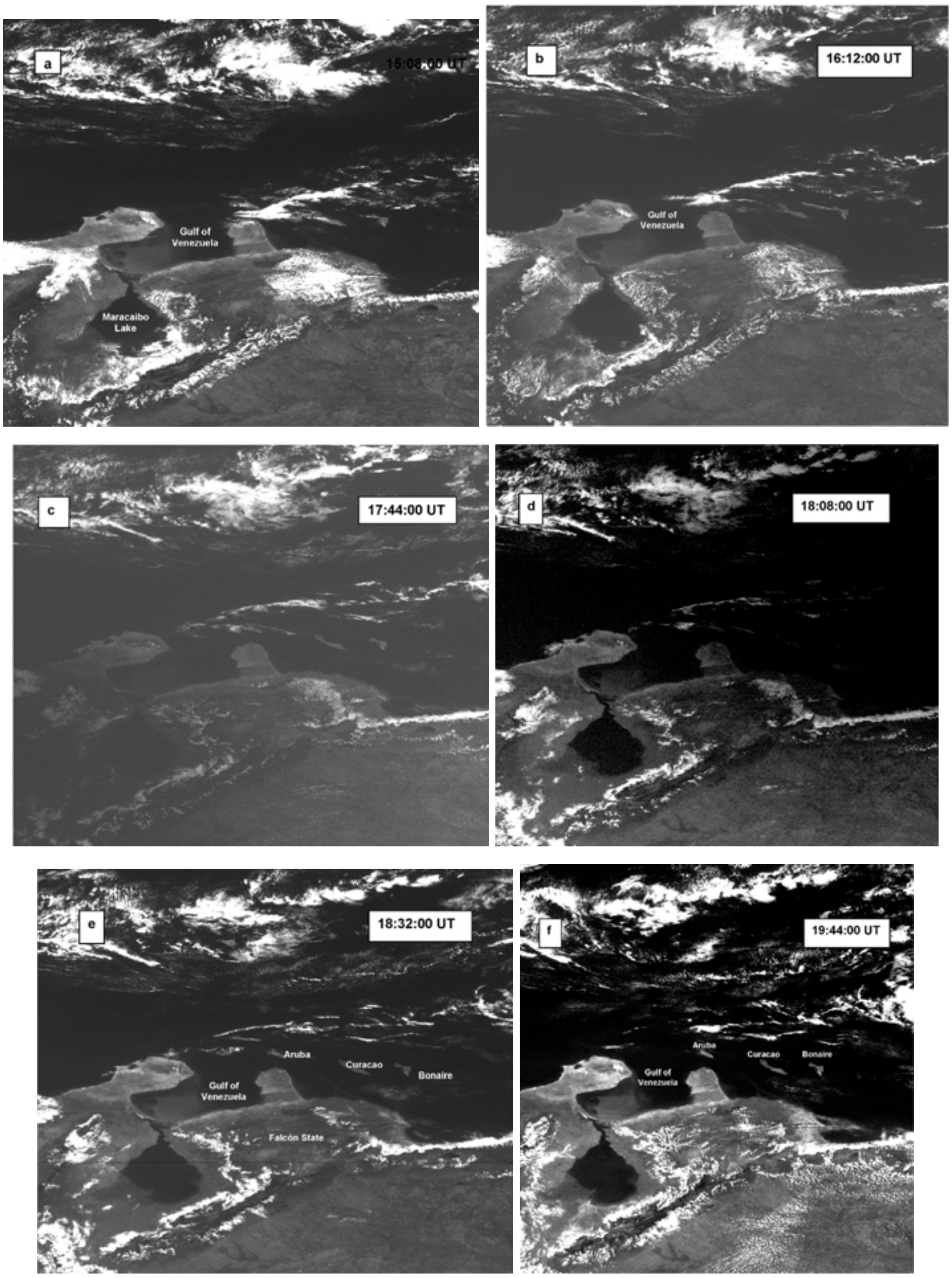

Figure 5. Sequence of six satellite images taken on 26th February 1998 of western Venezuela by the NASA satellite GOES-10, including Paraguaná Peninsula, showing the cloudiness variation at different times. The zone remained practically with clear sky. In (c) the shadow is seen falling to the west before crossing the peninsular area, and in (d) the shadow is crossing it. The penumbra is also seen in these pictures (images courtesy of NASA).

area, hemispherical field-of-view (∼180°), in combination with a photopic filter (400–700 nm), both used with an EEO Research Radiometer/Photometer unit. The photosensors were calibrated at Essex University before they were taken to Venezuela (Peñaloza, 1999). To perform this, a Wotan Xenophot HLX quartz diffuser bulb, with a tungsten filament, was used as a light source, and to compare, a LI-COR integrating quantum/radiometer/photometer, model LI-188B was also used. Different glass neutral density filters were applied in the calibration procedure in order to obtain the respective calibration curves in kilorayleighs (kR). All photosensors during calibration were illuminated totally to account for the wide field-of-view of two of them.

The rayleigh, a photometric unit introduced by Hunten et al. (1956) for the airglow and aurora, has been almost universally adopted by experimentalists in aeronomy (Baker and Romick, 1976). Also it has been adopted in contemporary works dealing with the sky brightness during solar eclipses (Sharp et al., 1966; Dandekar, 1968; Velasquez, 1971; Dandekar and Turtle, 1971; Lloyd and Silverman, 1971; Miller and Fastie, 1972; Carman et al., 1981). Historically, the rayleigh unit was defined as an emission rate of 1 million photons per second from an extended column of 1-cm cross (Baker and Romick, 1976). In SI units this is equal to 10^{10} photons s^{-1} m^{-2} per column. As stated by Baker (1974) the justification to use a radiance (or surface brightness) unit like this relies on the fact that in gaseous photophysics the photon is conveniently treated statistically along with the concentration of the other particles of the medium; this unit gives a measure of the rate at which photons coming down from a region of the sky would strike each square centimetre of normal area per time unit, and the word "column" is inserted to convey the idea of an emission-rate from a column of unspecified length. The factor to convert photons per second into watts of light energy is simply hc/λ times the photon rate, where the constants have their usual meanings and λ is the wavelength. For a full appreciation of this unit and further details, the reader is referred to the works by Baker (1974), and Baker and Romick (1976).

In the *in situ* experimental procedure, and by applying the corresponding eclipse map given by Espenak and Anderson (1996), an arrangement of the three photosensors was set up so that the Macam's, covered with a white diffuser size of 64 mm^2, pointed to the horizon, perpendicular to the totality path (altitude 0°, azimuth 150°); the EEO's also to the horizon but anti-parallel to the totality path (altitude 0°, azimuth 240°); the RS's, covered with a white flashed opal glass diffuser of 25 mm diameter, to the zenith. This direction determined that this photosensor (device diameter, 8.26 mm) was housed in a cylindrical black case, 57.88-mm height and 25.66-mm width (for a narrow field-of-view of 17.1°). Previous technical checking against the horizon and zenith during a normal day (see below), and based on the fact that it has been noted that in past total solar eclipses the horizon is brighter than the zenith, showed that the appropriate distribution and setting of the photosensors was that referred to above. Because the horizon detectors have wide field-of-view it was not necessary to measure exactly their altitude within a degree precision.

Otherwise, with small field-of-view detectors, the exact altitude of the instrument should be stated to the nearest degree since a precise knowledge of this parameter is vital for any comparison with models; the sky brightness vary greatly with even the change of one degree in altitude near the horizon.

The arrangement was installed in the roof of the booster radio station water tank supply, high enough over the ground to have a good view all over the horizon. The photosensors were directed inland, opposite the sea. In this way the predominant surface albedo was that corresponding to a semi-desertic ground. Buildings belonging to the booster station and other obstacles in different lines of sight to the sea prevented the horizon photosensors from pointing in those directions. The zenith distance of the Sun during the eclipse was quite enough apart so that it was not necessary to screen it in order to carry out the zenith measurements. Due to the light colour of the water tank roof's surface, care was taken to put the photosensor arrangement just on one edge of the roof in order to avoid possible interference of the shadow bands which were abundant after the third contact according to unaided eye observations made on this surface.

4. Observations

The output signal measurements from the sensors were simultaneously acquired with a data-logger, at a rate of one reading per minute per channel for six hours (from 11:00 am to 5:00 pm), to cover part of day light under normal or noneclipse conditions for reference purposes. The resolution value of 1 μA corresponding to the channel used to acquire the current signal from the Macam sensor, prevented from measuring signals below this quantity. Therefore minimum values related to these measurements during the totality, which were below this limit, had to be interpolated by using the second and third contact values, respectively.

Figure 6 shows the profile of the horizon sky brightness perpendicular to the shadow path obtained with the Macam sensor, in the wavelength range of 400–700 nm, from 11:00 am to 5:00 pm Venezuelan local time. As can be seen the stability of the device was very good as it was for the other instruments. This brightness is presented along the ordinate on a logarithmic scale in the unit of kR, and the minimum value obtained during the totality was approximately 6×10^2 kR.

The horizon sky brightness profile obtained with the EEO detector in the direction of the shadow path but opposed to it (anti-parallel) are shown in Figure 7. As in Figure 6, this brightness is presented on a logarithmic scale in kR. Between 13:38 and 14:35 this sensor caught some significant spurious or extraneous signals of unknown origin (some of which, in turn, were also detected by the Macam sensor in a lesser magnitude and removed from the raw data) whose origin or source could not be identified. James (1998) measuring the zenith sky brightness at the same location (Punta de Barco) with a portable luxmeter but with hemispherical view also obtained some offset points during the totality. These spurious signals also

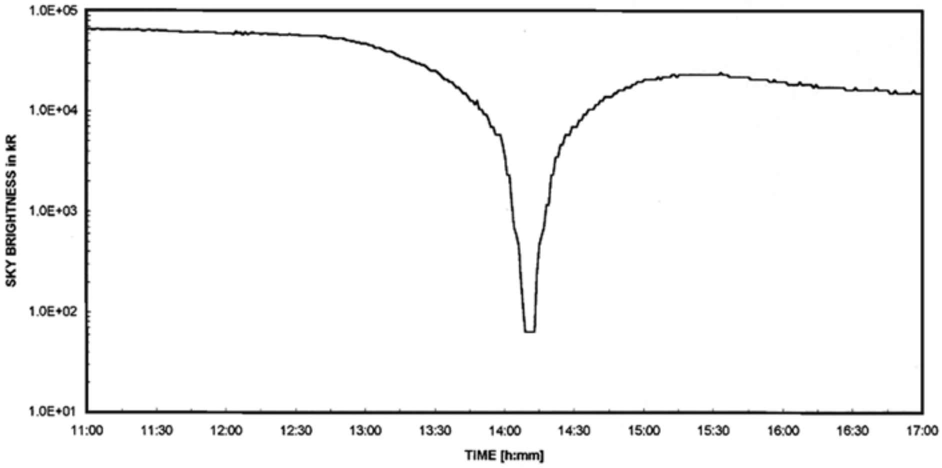

Figure 6. Plot showing the horizon sky brightness profile perpendicular to the shadow path obtained with the Macam sensor, in the wavelength range of 400–700 nm, from 11:00 am to 5:00 pm Venezuelan local time.

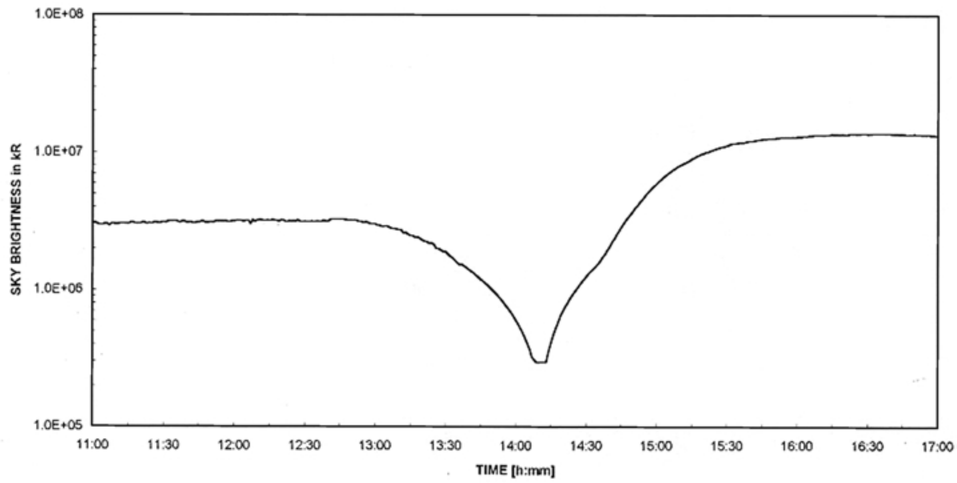

Figure 7. Plot showing the horizon sky brightness profile obtained with the EEO detector in the direction of the shadow path but opposed to it (anti-parallel), in the same wavelength range (photopic), and in the same time period, as in Figure 6.

had to be removed from the raw data of this sensor. Yet in this case, however, by using the second and third contact again, values corresponding to this period including those during the totality were extrapolated and interpolated, respectively. In this case the minimum value obtained for the totality was approximately 3×10^5 kR.

Figure 8 shows the profile corresponding to the zenith sky brightness in the same units, obtained with the RS photosensor in the wavelength range of 300–

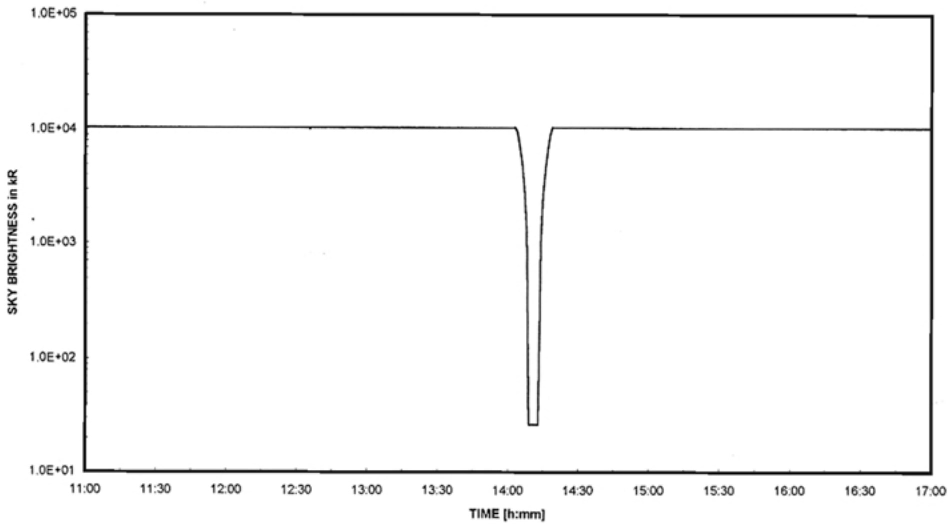

Figure 8. Profile of the zenith sky brightness obtained with the RS photosensor, with a narrow field-of-view, the wavelength range of 300–1200 nm, and in the same time period in Figure 6.

1200 nm. During the totality the minimum value obtained for this celestial point was approximately 2.7×10 kR.

Percent obscuration at the ground level is presented for the zenith curve at the top axis of Figure 9, for a period of about 16 min that includes second and third contacts.

5. Extinction Coefficient and Optical Depth Estimations

A direct estimation of the total extinction coefficient in the visual, k_g [in mag/air mass (defined below)], towards the zenith due to the contributing components, is given by

$$k_g = k_R + k_a + k_{oz} + k_{wv}, \tag{1}$$

where k_R is the Rayleigh scattering component, k_{oz} is the ozone component, k_a is the atmospheric aerosols component, and k_{wv} is the water vapour component. In general, for other directions it is more complicated, and the extinction coefficient as defined by Schaefer (1993) should be taken into account. However, for all but low horizon observations, an approximate usage of Equation (1) is adequate to describe the general state of the atmosphere because the air masses are basically identical for all components when the horizon area is avoided. Hence k_g will be called the global total extinction coefficient. Then the components, given in Equation (1), according to Schaefer (1993, 1998), are

$$k_R = 113700(n-1)^2 \exp[-H/H_e)]\lambda^{-4}, \tag{2}$$

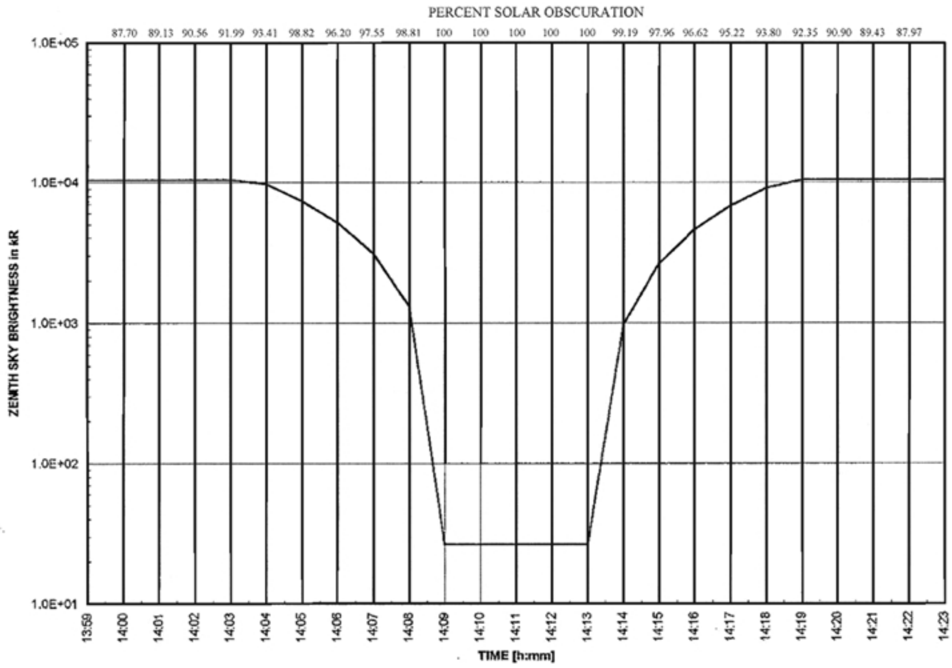

Figure 9. Zenith sky brightness as a function of the percent solar's disk obscuration (top axis) by the Moon, at the ground level, for a central period of 22 min around the total phase that includes the second and third contacts.

$$k_{oz} = (0.031/3.0)\{3.0 + 0.4[\phi \cos(\alpha_s) - \cos(3\phi)]\}, \quad (3)$$

$$k_a = 0.12[0.55/\lambda]^{1.3}[1 - (0.32/\ln S)]^{4/3}[1 + 0.33 \sin(\alpha_s)] \exp(-H/1.5), \quad (4)$$

$$k_{wv} = 0.94 W_\lambda S \exp(t/15) exp(-H/8200). \quad (5)$$

In Equations (2)–(5), n is the index of refraction at sea level, λ is the wavelength (in microns), H is the observer's height (in km) above sea level, H_e is the scale height (in km), ϕ is the observer's latitude (in radians), α_s is the right ascension of the Sun, W_λ is a function of the wavelength, t the air temperature (in °C) and S is the relative humidity. Equation (5) can be found in Schaefer (1998). A stellar magnitude, mag, is a logarithmic unit of intensity, where one magnitude corresponds to roughly a factor of 2.52 in brightness regardless in what units the intensity is given. This is the basic unit of brightness used by astronomers; if I is an intensity, the magnitude is defined by the expression $C - 2.52 \log_{10} I$, where C is an arbitrary constant (Young, 1990; Hearnshaw, 1992). In general, on the other hand, the unit of atmospheric distance is given by the local relative optical path length, which is defined as the ratio of the optical path length along any trajectory to the vertical path length in the zenith direction (one air mass). Therefore the units of astronomical extinction are magnitudes per air mass (mag/air mass); one magnitude per air mass equals 2.52

$\log_{10}e$ ($\cong$1.086) optical depths per air mass (Taylor et al., 1977; Bruin, 1981) (see Equation (13) below).

It is well known that atmospheric aerosols come from many sources (sea spray, windborne desert dust, etc.). Fortunately there are a variety of trends which can be used to provide a reasonable guess for the aerosol extinction coefficient, k_a. Thus Equation (4) is based on an evaluation of trends for time of the year, relative humidity, altitude, and wavelength. Additional sources of extinction such as volcanic aerosol layers and urban pollution, not included in this analysis, have to be treated, respectively, in a different and appropriate manner. Schaefer (1993) states that the use of the equations above allow for the extinction to be reasonably estimated for any site in the world provided that urban areas and special situation of volcanic events are not included.* Therefore for application purposes of this model, it must be stressed that only a remote or a semi-remote site has to be considered.

Therefore for Rayleigh scattering $H_e = 8.2$ km (Allen, 1973). For visual wavelengths ($\lambda = 0.55$ μm), and for Punta de Barco site in particular, these equations are reduced to:

$$k_R = 0.1066, \tag{6}$$

$$k_{oz} = (0.031/3.0)\{3.0 + 0.4[0.21\cos(\alpha_s) - 0.80]\}, \tag{7}$$

$$k_a = 0.12[1 - (0.32/\ln S)]^{4/3}[1 + 0.33\sin(\alpha_s)], \tag{8}$$

$$k_{wv} = 0.029S\exp(t/15). \tag{9}$$

By applying Equation (1), taking into account Equations (6)–(9), k_g can be found for the atmosphere of this particular location during the day of the eclipse. To find α_s calculations with the *AstroScript* software provided by Duffet-Smith (1997) were performed. The values for S and t were taken from the data published in the ARVAL Observatory web site, whose team was in the same location making meteorological observations. Figure 10 displays the variation of the relative humidity (in %) on 25/02/98, from 07:30:00 to 17:30:00 (local time), and on 26/02/98, from 09:30:00 to 17:30:00 (local time), and Figure 11 displays the same variable during the whole eclipse, from 12:42:00 to 15:39:00 (local time). Figure 12 presents the temperature measurements made the day of the eclipse also by the ARVAL Observatory.

* Indeed the aerosol density can vary by large factors. But the bulk of the variance arises due to effects of altitude, relative humidity, and time of year. Equation (4) incorporates these effects by giving the equations for the best correlation between the quantities involved. When these correlations are accounted for, a large fraction of the variance in the "standardized" aerosol density (i.e., standardized to sea level, zero relative humidity, temperate northern latitudes, and near the equinoxes) is eliminated. Even so, there can still be large variations around the best value of the specific equations involved due to manmade pollution, forest fire, volcanoes, etc. Nevertheless, from a very large data base with $>10^5$ measurements from >300 sites worldwide, the scatter of Equation (4) is remarkably good (B. Schaeffer, personal communication, 1999).

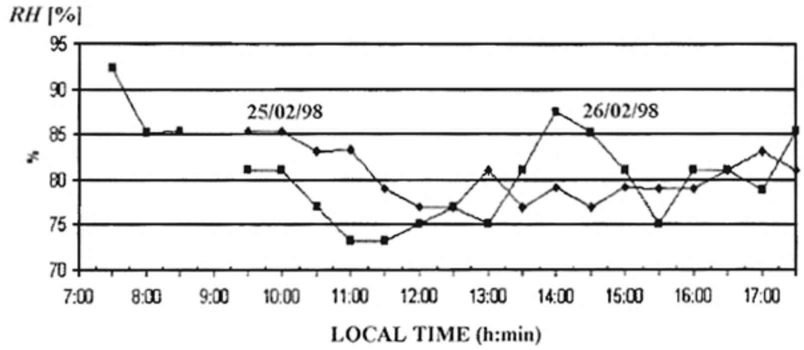

Figure 10. Variation of relative humidity the day before (25/02/98), from 07:30 to 17:30 (local time), and the day of the eclipse (26/02/98), from 09:30 to 17:30 (local time), measured by the ARVAL Observatory at Punta de Barco (Paraguaná Peninsula, Falcón, Venezuela).

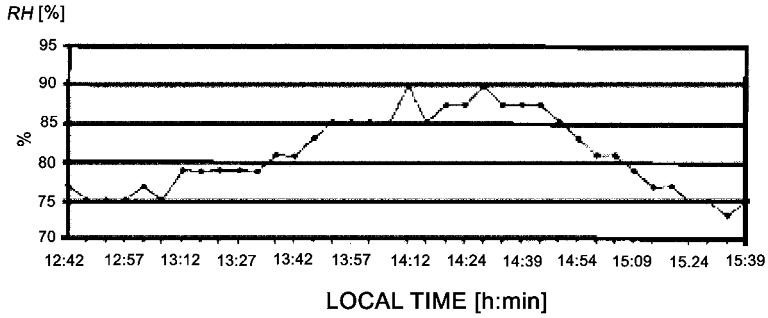

Figure 11. Variation of the same variable as in Figure 10 but during the whole eclipse, from 12:42 to 15:39 (local time), measured by the ARVAL Observatory at the same location as in Figure 10.

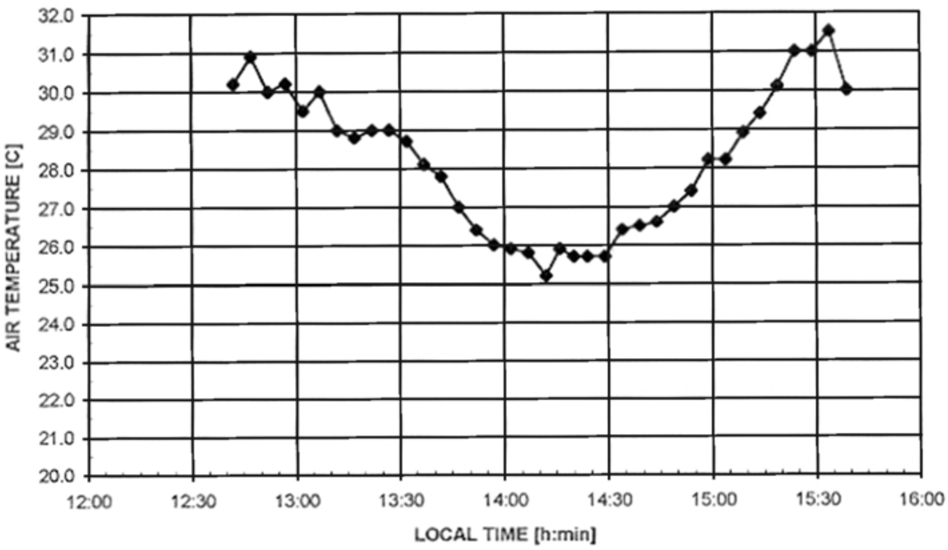

Figure 12. Variation of temperature during the eclipse between 12:42 and 15:39 (local time), measured by the ARVAL Observatory at Punta de Barco (Paraguaná Peninsula, Falcón, Venezuela).

It is important to note that the primary analysis of this paper is not to calculate, in a particular direction, the extinction coefficient, k, via photometric measurements of the sky brightness by applying Equation (13). However, they can in principle be useful to explore this possibility in the way described next.

Being the horizon direction unacceptable for the aforementioned model, the photometric measurements made of the horizon sky brightness under noneclipse and eclipse conditions could be used to estimate, in a rough way, the extinction of the atmosphere (and its corresponding optical depth) in this particular direction along that day, using a photometric model presented by Schaefer (1993). By experience it is well known that these parameters can vary quite widely with altitude and azimuth as well as from hour to hour, from minute to minute, and so on, within a given day. So the best that can be done is to use an average value to represent the sky conditions for a given date and direction.

Ideally, the sky brightness should be calculated taking into account multiple scattering. However in a first approximation, according to Schaefer (1993), a semi-quantitative estimation of the cloudless sky brightness in nanolamberts (nL) during daylight can be given to 20% accuracy by,

$$B_{\text{day}} = N_\lambda f(\rho_{\text{sun}}) 10^{-0.4kX(Z_{\text{sun}})}[1 - 10^{-0.4kX(Z)}], \tag{10}$$

where k is the total extinction coefficient, defined here in units of stellar magnitudes per air mass; Z_{sun} and Z are the zenith distance of the Sun, and the sky direction, respectively; ρ_{sun} is the separation between the sky direction and the Sun; $X(Z_{\text{sun}})$ and $X(Z)$ are the respective air mass functions; N_λ is a coefficient depending on wavelength λ (for the visual it is equal to 11,700); and $f(\rho_{\text{sun}})$ is an approximate scattering phase function given by Krisciunas and Schaefer (1991),

$$\begin{aligned} f(\rho_{\text{sun}}) &= 10^{5.36}[1.06 + \cos^2 \rho_{\text{sun}}] + 10^{6.15-(\rho_{\text{sun}}/40 degree)} \\ &\quad +6.2 \times 10^7 (\rho_{\text{sun}})^{-2}, \end{aligned} \tag{11}$$

with ρ_{sun} measured in degree. This function gives values much too high for small values of ρ_{sun}. Schaefer (private communication 1999) suggests that for $\rho_{\text{sun}} < 20'$ it should be replaced by a different expression (note that the angular diameter of the Sun is about $\sim 32'$ at mean Earth distance so in fact for $\rho_{\text{sun}} < 15'$ the Sun is being looked at). Therefore for the purpose of the present work, in which values of $\rho_{\text{sun}} \gg 15'$ are involved, the use of Equation (11) is sufficiently valid.

For altitudes near the horizon, but not below,

$$X(Z) = [\cos Z + 0.025 \exp(-11 \cos Z)]^{-1}, \tag{12}$$

is a convenient and a fairly good approximation for reasonable elevations above sea level and aerosol density (Rozenberg, 1966).

Given the values of B_{day} obtained from the photometric measurements, and by solving numerically Equation (10), approximate values of k were found for different values of the other parameters calculated from Equations (11)–(12). Then the results can be used to estimate the optical depth (in any direction Z) for different values of k by applying,

$$k = 1.086\tau, \tag{13}$$

where k is given in mag/air mass, and τ is the optical depth (Schaefer, 1993); this optical depth depends, in a proportional manner, on the geometrical path, air density, characteristics of components, and sec Z. By comparison, the difference between the extinction coefficient given by Equation (1) and that given by Equation (13), can be distinguished.

Although Equation (10) is transcendental for k, it could be solved for most of the input data by applying a computer code. To find values of Z_{sun} the *AstroScript* software by Duffet-Smith (1997) was used. Because the angle ρ_{sun} was available only for the horizon anti-parallel direction (opposite the shadow path), the calculation of k was only possible for that particular direction. Zenith direction was not considered since during total solar eclipses, second order scattering plays an important role in the zenith sky brightness (Figure 3). Although in Equation (10) the two terms involving powers of ten account for not only the case of single scattered light but also for double scattered light, the term representing the phase function [Equation (11)] only account for single scattering; therefore, Equation (10) cannot be applied to the zenith direction.

Note that Equation (10), through the factor N_λ, is wavelength-dependent. Thus an integral over the spectral responsivity of the detector must be made. Also this equation is dependent on direction; using a wide field-of-view detector an integration over sky position in the field of view must be made. Finally, it is emphasised that the changing sky brightness during the totality is primarily due to varying fractions of atmospheric illumination within the penumbra; therefore, any comparison can only be correctly made with a detailed model involving the multiple scattering of light and the geometry of the specific eclipse. However by taking into account that the photometric measurements made with the EEO's sensor were integrated in the visual range (400–700 nm), a value of 11,700 for N_λ is given for this range (Schaefer, 1993). By its wide field-of-view, the detector considered (EEO) also integrates in a hemispherical way the light over the sky position. However considering that the sky brightness decreases from the horizon to higher altitudes (except in that area close to the Sun) (Jeske, 1988), and that the sensor collects the light on the horizon between 0° and 180° on this plane but in altitude only between 0° and 90°, the light mostly comes from the horizon. Thirdly, a single scattering process in the penumbra produces much of this light. In this manner, the values of B_{day} to be used in Equation (10) are instrumentally integrated and the corresponding values of k can potentially be interpreted as a rough estimate of this parameter in that direction, in that spectral range. For qualitative purposes these values can be considered suffice to outlook the variation of the extinction coefficient in the visual and in the specified direction. In the calculations a conversion factor of 47.6 nL/kR was applied which was obtained from the data given in Table II of the paper by

Dandekar (1968). There it is stated that 0.9 mL is equivalent to 21.0 kR/Å; taking into account that the effective width of the visual is ~900 Å, 1 kR = 9 × 10^5 nL/(900 Å × 21 kR/Å) = 47.6 nL. As it is known, one lambert is equal to one lumen (lm) per square centimetre and a lux (lx) is one lumen per square metre. The latter has recently been used by Shiozaki et al. (1999), Darula and Kittler (2000), and Darula et al. (2001) in their papers related to variations of daylight during solar eclipses. In other recent paper on sky brightness when the sun has been in eclipse at dawn, the candle per square metre unit has been used by Liu and Zhou (1999). This demonstrates that photometric measurements and their units, in its different forms, continue nowadays being used to study the sky brightness during solar eclipses since the first reliable instrumental observations of this type were made in the last quarter of the ninetieth century by Abney and Thorpe (1889); moreover, these are justified when they have to be associated to visual observations (as in this paper).

In order to have a conversion factor from any of these units of luminous flux to radiant flux (i.e., [lm W^{-1}]), a quantity called luminous efficiency of the radiation has to be defined which, in turn, depends on wavelength (Middleton, 1952). For example, it has a value of 685 lm W^{-1} at 5550 Å (McCluney, 1968). The method to obtain the integrated factor, as well as other conversion factors between radiometric-photometric units, implies an integration process over the wavelength range of interest which takes into account this efficiency and the specific radiometric quantity involved. For further details the reader is referred to Lovell (1953), Meyer-Arendt (1968) and McCluney (1968) who give basic comprehensive treatments on this matter.

6. Results, Discussion and Analysis

Due to the different sensors used and their variability in solar wavelength sensitivity span and spectral response, a strict intercomparison among these curves is not possible. Nonetheless some useful information can be obtained. First of all with the support of Figure 7, it can be estimated that the horizon sky brightness is reduced by about three orders of magnitude as compared with that due to the uneclipsed Sun during the morning and also during the afternoon. Note that the curve is not symmetric around the midtotality. Given the specific direction involved (perpendicular to the Sun track vertical plane) this is a consistent feature because in normal conditions the horizon sky brightness had decreased steadily, from the morning until late in the afternoon. The minimum value observed in this case during the totality was approximately 7 × 10 kR (70 kR). For comparison note that the brightness of the night sky is about 250 R (0.250 kR) and the aurora lies between 1 and 1000 kR (Jerrard and McNeill, 1986). Therefore the horizon sky brightness in this particular direction, and during the totality, turned out to be ∼ 280 times brighter than that of the night sky, or alternatively, ∼ 36 times brighter than that of the typical sky at full Moon. The maximum value observed during the morning (pre-eclipse) was

$\sim 6.5 \times 10^4$ kR, and the maximum value during the afternoon (post-eclipse) was $\sim 2.2 \times 10^4$ kR which are values, in order of magnitude, near those typical of the brightness for a normal day light clear sky (6.95×10^5 kR). This indicates that the horizon sky brightness in that direction, and under noneclipse conditions, was 10 times less bright than that of a typical daytime. Taking the maximum (noneclipse condition) and minimum (totality) values as references, the reduction in brightness was a factor of 10^3. This kind of reduction has been observed by Dandekar and Turtle (1971) during the total solar eclipse on 7 March 1970, at solar azimuth 180° and a distance 90° away from the Sun, at 630 nm wavelength.

From Figure 7, it could be estimated that the horizon sky brightness, opposite the umbra path, is reduced by only one order of magnitude as compared with that due to the uneclipsed Sun during the morning and also the afternoon. It is convenient to bear in mind that this is the direction containing the Sun track vertical plane. During the morning this direction is opposed to the Sun, and during the afternoon it is approximately in the direction of the area just below the Sun. The curve is not symmetrical around the midtotality but it is inverse to that of Figure 6. The sky brightness on a normal day increases from that particular direction as long as the Sun is going down towards its sunset. The minimum value estimated during the totality was approximately 2.4×10^5 kR. The maximum value observed during the morning (pre-eclipse) was $\sim 3 \times 10^6$ kR, and during the afternoon (post-eclipse), $\sim 1.5 \times 10^7$ kR. In comparing these two latter figures with that of a typical daytime sky, it is noticed that in this particular direction the horizon was brighter than that of a typical daytime sky by a factor of 10 and 10^2, respectively. However this last factor is possibly enhanced to this order of magnitude due to a significant contribution of the direct solar radiation arriving at the detector, given the direction considered which is, during the afternoon, towards the sky area below the Sun.

From Figure 8, the zenith sky brightness has a reduction of about three orders of magnitude as compared with that due to the uneclipsed Sun. This reduction is similar to that obtained for the horizon perpendicular to the shadow path. Recalling that the Sun never was into the field-of-view of the RS detector (17.1°/2 = 8.55°), the maximum zenith sky brightness pre- and post-eclipse was $\sim 10^4$ kR during the period covered, indicating that this brightness was constant throughout the period covered for the uneclipsed Sun, that is to say, regardless of the position of the Sun. This is consistent with the zenith sky brightness measurements made by Dandekar (1968), Velazques (1971), and Shaw (1975). For the totality, the minimum value was $\sim 2.7 \times 10$ kR (27 kR) being approximately 108 times brighter than the night sky, or alternatively, $\sim$14 times brighter than that of the typical sky at full Moon. This last result is quite consistent to that obtained by James (1998) who inferred that the zenith sky brightness at the same location (Punta de Barco) was equivalent to $\sim$10 times the full Moon sky brightness. Silverman and Mullen (1975) reviewing the sky brightness during eclipses consider many related possibilities as references; among them are: photometric results, star sightings, twilights, comparison with moonlight, and visibility of printed or written letters, instrument parts, and objects.

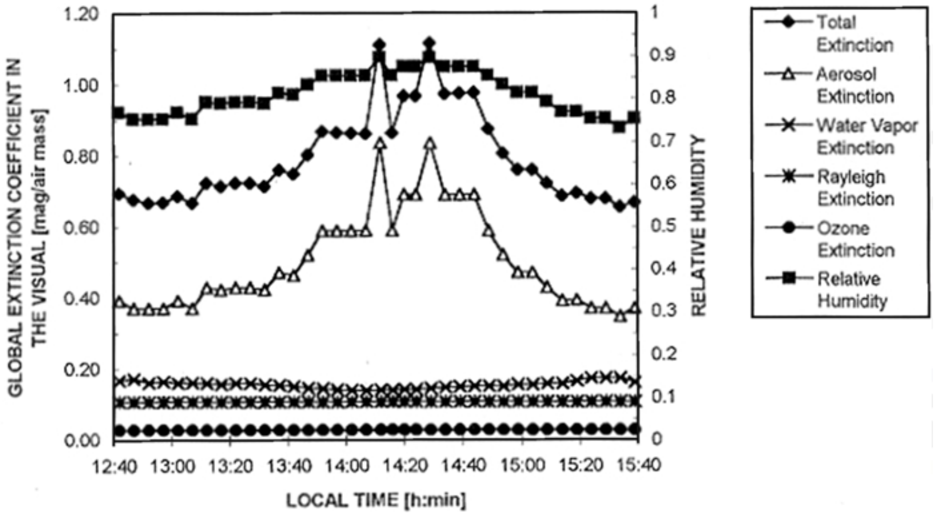

Figure 13. Profile of the global total extinction coefficient in the visual and those for each component contributing to it, between the first and fourth contacts, calculated from meteorological data provided by the ARVAL Observatory and using an empirical model by Schaefer (1993), at Punta de Barco (Paraguaná Peninsula), Venezuela. Note that the total profile is controlled by the aerosol profile. The water vapour profile is also included for comparison purposes.

They state that an estimate of the brightness ten times that of a full Moon is, of course, considerably less than the true value. Thus it is reasonable to think that the result obtained in this work is more reliable. Ignoring this discrepancy it can be said that the zenith was somewhat brighter than a typical full-Moon-sky.

From this result quoted it can be noticed that the zenith brightness turned out to be less bright than the horizon which, in turn, is a result consistent with those obtained in past total solar eclipses. In particular, it has been found that the horizon perpendicular to the shadow path is approximately 2.6 times brighter than the zenith. This result is very similar to that found by Schaefer (1986) who studied the brightness of the night sky (roughly twice) for a set of "standard" observing conditions at Cerro Tololo Interamerican (Chile) and Kitt Peak National observatories. From Figure 9 the brightness begins to change just 6 min preceding and following the totality. In terms of solar obscuration, this change begins to occur when the solar disc has been obscured by 91.99%. In terms of solar brightness it begins to appear when the sun magnitude has fallen by 3 units, approximately, few minutes before the onset of totality at second contact (Hughes, 2000). Yet this change is even more drastic when this percentage yields 98.81% as can be seen in this figure. Below this value effects associated with total solar eclipses can be interpreted in terms of attenuated, but otherwise essentially unchanged Sun (Sharp et al., 1971).

Figure 13 shows the profile of the global total extinction coefficient in the visual, k_g, and those for each component contributing to it, between 12:42 and 15:39 (local time), are also shown. It is evident that the aerosol is the main contributor to this coefficient in comparison with the other two (water vapour, Rayleigh and ozone extinction) so that $k_a \gg k_{wv} > k_R > k_{oz}$. It is also seen that it is strongly dependent on relative humidity (see Figure 11) which rises during the totality and just after it (see Figures 10 and 11). This last feature is consistent with observations made of relative humidity in past eclipses (Ugueto, 1916; Brooks et al., 1941; González, 1997). The calculation of k_g in the way shown by Equations (1), (6)–(9), is very useful because it gives an estimation of the general darkness of the sky during the totality. Table I presents values for k_g, for seven different situations at night, taken from Schaefer (1986). Note from this table that a very poor night has a $k_g = 0.50$ mag/air mass; from Figure 13 it can been seen that, for example, at 14:07 (local time) this coefficient increased to a value of 0.86 mag/air mass, and for 14:12 a value of 1.11 mag/air mass was obtained, indicating a very poor "night" during the totality. In fact only Mercury, with an apparent visual magnitude (m_V) of -0.2, Jupiter ($m_V = -2.6$) and Venus ($m_V = -4.22$) were seen clearly close to the Sun by this author, and only two stars, Deneb (α Cyg) with $m_V = 1.25$ (Allen, 1973), and Fomalhaut (α PsA) with $m_V = 1.16$ (Allen, 1973), were reported present, respectively, by Schaefer (1998), on Aruba island very close to the Paraguaná Peninsula, which can be seen on the horizon from Punta de Barco (actually 31 km off the peninsula coast; see Figure 2), and by the ARVAL Observatory at this last observation site. According to the criterion given by Silverman and Mullen (1975) a dark eclipse can be qualified as such if stars of third magnitude ($m_V = 3$) can be observed. In comparing the above reported star sightings with this criterion, it is certain that the eclipse here was not dark at all even in the centre line of the path where the observation site was located. It is expected that this limit decreases due to a dependence of it on the distance to the nearest edge of the shadow.

The most probable cause explaining the results reported in this work resides in the influence of the aerosol contained in the troposphere, on the scattering of light coming from the penumbra and in the umbra itself (see Figure 3). It is well known that some of atmospheric aerosol species are hygroscopic, and their optical properties are a strong function of relative humidity (Hegg et al., 1993; Tang, 1996). As this parameter increases during the total phase of a solar eclipse leading to a decrease in water vapour content of the air (Bose et al., 1997), the water uptake by aerosols also increases, and the scattering of light by them likewise. This can explain the fact that the extinction coefficient of aerosols increases during the totality of an eclipse of the Sun, increasing the sky brightness at the same time. Moreover the Paraguaná Peninsula ($\cong$2396 km^2) is a semi-arid zone connected to mainland through a very narrow isthmus or strip of land 30 km (18 miles) in length by 5 km (3 miles) in width, called the Isthmus of the Medanos (Figure 2). It is arid but with some parts constituted by big and tall shifting sand-dunes called the Medanos of Coro (Coro city is the capital of Falcón State) that have been formed by the gusting east winds. The tallest of these "Medanos" can reach heights over 25 m (81 ft), along the isthmus (as well as a small section of the continental coast nearby). Possibly the natural aerosol background of the region

TABLE I

Global extinction coefficient values for different ambient conditions (Schaefer, 1986)

k_g (mag/air mass)	Description
0.10	Best night on dry mountain top
0.15	Average night on dry mountain top
0.20	Poor night on dry mountain top
0.20	Best night at dry sea level site
0.25	Average night at dry sea level site
0.25	Best night at humid sea level site
0.30	Average night at humid sea level site
0.40	Average night at poor site with much dust or humidity
0.50	Very poor night

These descriptions are provided so that estimates of the average can be deduced in the absence of better data. Variations around the stated mean will occur at different sites, times of day, and times of year. A "dry sea level site", for example, may have quite clear skies or it may have morning hazes or it may have substantial amounts of windborn dust. The user should guard against known climate change.

is a mixture externally composed of marine hygroscopic aerosol and dust particles from these sand-dunes aloft with a high scattering altogether. During the eclipse the effect referred to above could have been enhanced by an additional increase of the normal aerosol background of the zone, due to the presence of thousands of cars, coaches, and other motor vehicles which visited the Peninsula. It seems probable that it could contribute to make the aerosol internal mixture more complex but not enough to increase appreciably the aerosol concentration in the area as to be considered highly polluted.

It is interesting to note that a few previous works have been enough to demonstrate the influences of the meteorological parameter changes upon atmospheric aerosol properties as a consequence of solar eclipses.

Perhaps Maske et al. (1982), Manohar et al. (1985), and Fernández et al. (1993) were the first authors in revealing direct and indirectly these influences, in particular, from the solar eclipse of 16 February 1980 in India (Fiala and Lukac, 1978; Bhattacharyya, 1978; Maske et al., 1982; Manohar et al., 1985) and from the solar eclipse of 11 July 1991 in Costa Rica (Fernández et al., 1993).

In the report of Maske et al. (1982) observational results are presented indicating that an increases of the concentration of suspended particulates was detected during this eclipse, being well above the usual range of suspended matter in clean mountain air. In the same event, from the lowered atmospheric conductivity measurements made at Raichur by Manohar et al. (1985), they suggested the formation of small particles due to high humidity conditions by the eclipse forcing as the explanation for the atmospheric conductivity decreases and the subsequently increasing in the atmospheric electric field: in the presence of such particles, small ions are lost through diffusion over the surfaces of these particles leaving large ions that produce a shift in the size distribution from small ions to large ions.

Interestingly, from the measurements made by Fernández et al. (1993) of direct solar radiation during the 1991 solar eclipse in Central America (Fernández et al., 1992), they were able to deduce an increasing of aerosols in the atmosphere through an analysis of the Ångstrom's parameters (turbidity coefficient β and growth exponent α), thus corroborating the finding of Maske et al. (1982). As a response to the totality these parameters acquired unusual values varying in opposite directions, β rising and α diminishing in the indicated interval. According to their explanation this is indicative of a presence of a high number of large particles in comparison with a low number of small particles. As mentioned above, they agree that aerosols may have been salt particles from the sea and dust particles from the ground. The efficiency of such particles as condensation nuclei depends on their properties. Hygroscopic particles are of special interest: When RH is high, they absorb water and grow. Therefore, their size augment during the eclipse as temperature falls sensibly; as a result, RH rises in a comparatively short time, effect this that, in passing and historically speaking, was already noted as early as 1927 precisely in the solar eclipse of 29 June but at Jokkmokk, northern Sweden, on the Arctic Polar Circle (Stenz, 1929).

Later reports on direct atmospheric aerosol measurements under solar eclipse situation correspond to Dani and Devara (1996), Sapra et al. (1997a,b), Niranjan and Thulasiraman (1998), Bansal and Verma (1998) and Singh et al. (1999) which dealt with the solar eclipse of 24 October 1995 also in India (Espenak and Anderson, 1994).

In the second and third of these works a 2–4 fold increases in the aerosol number and mass concentration, occurred mainly in the sub-micron size and after a time lag of about 80 min from the beginning of the eclipse, were reported at Bhabha Atomic Research Centre in Trombay where the phenomenon reached a partial maximum of 72% obscurity.

In the fourth one, Niranjan and Thulasiraman (1998), working with a network of 5 multiwavelength radiometers, detected an increases of the aerosol optical depth in a tropical site located on the east coast of India (Visakhapatnam) as a result of a change in the local meteorological parameters, associated with the reduction in the solar flux due to a total solar eclipse. Certainly this increases is related to a change in the optical properties of the coastal aerosol due to a change in the ambient relative humidity. They also reported a change in the aerosol size distribution. Similar results, found at Robertsgunj (Uttar Pradesh), were previously reported in the first of these works (Dani and Devara, 1996).

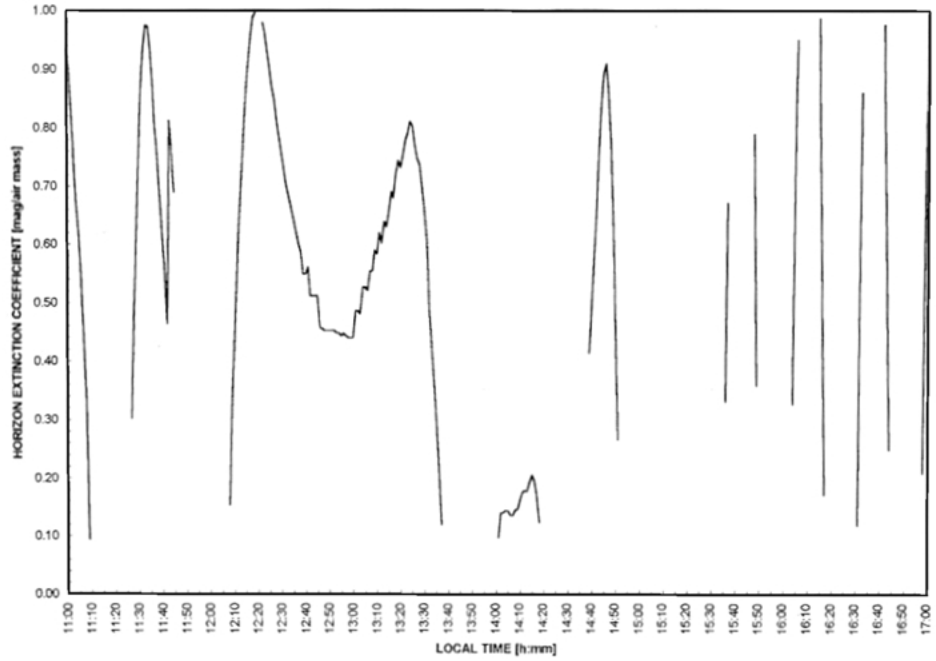

Figure 14. Variation of the extinction coefficient in the horizon direction, opposite (anti-parallel) the shadow path, between 11:00 and 17:00 local time, the day of the eclipse. The values are gross estimates. However this profile can portray or represent the variation of this parameter at that day, and in that direction. Note that during the total phase, and after the third contact (14:13:02, local time) an increase of the extinction coefficient was detected.

Observations made at Roorkee (90–92% maximum obscurity), described in the last two of these reports, also concluded that the aerosol concentration increased during the phenomenon.

Figure 14 depicts a general view of the variation of the extinction coefficient for the horizon direction, opposite (anti-parallel) the shadow path, between 11:00 and 17:00 local time. It fluctuates in an irregular way between 0.99 and 0.09 mag/air mass, the average being equal to 0.57 (∼0.60) mag/air mass. In general irregular fluctuating behaviour is typical for this coefficient in the troposphere, mainly in the boundary layer, on a daily basis. By applying Equation (13) a gross mean value of 0.55 for the optical depth was found in that particular direction along that day. Note that during the total phase, and after the third contact (14:13:02, local time) an increase of the extinction coefficient is detected as a consequence of the atmospheric response to the eclipse; this result is consistent with that obtained for the global total extinction coefficient at Punta de Barco (see Figure 15) and with that expected to happen during and just after this phase (Maske et al., 1982; Fernández et al., 1993; Dani and Devara, 1996; Sapra et al., 1997a, b; Niranjan and Thulasiraman, 1998).

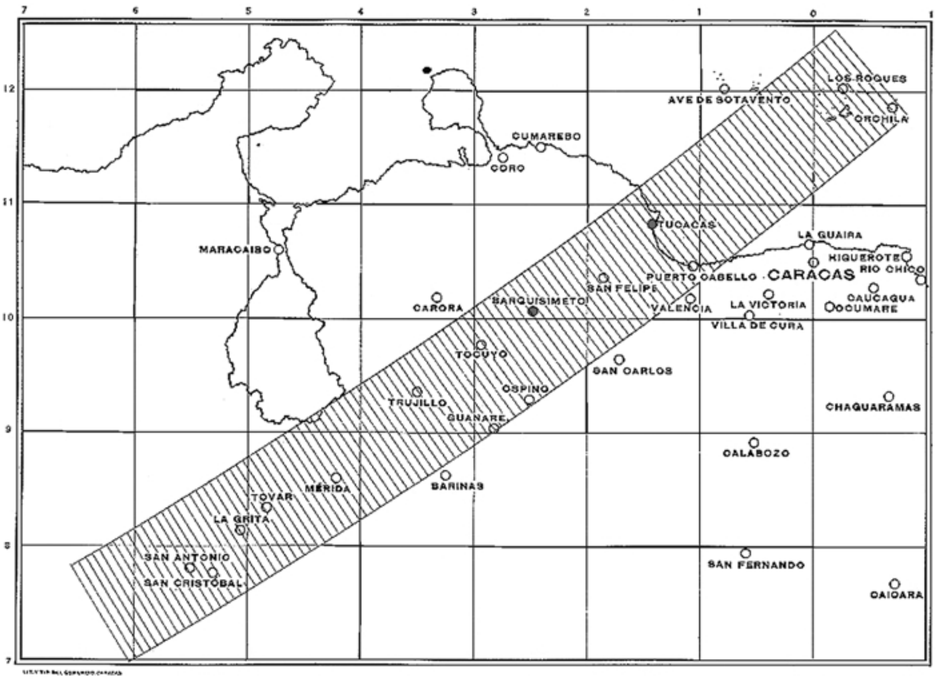

Figure 15. The shadow path of the total solar eclipse of 3 February 1916 through Venezuela. Tucacas town is located on the coast, and Barquisimeto city is about the centre of the map. Both are indicated as a black dot (map reproduced from Ugueto's report).

7. Comparison with the Total Solar Eclipse of 3 February 1916

As mentioned earlier, the total eclipse of 3 February 1916 was the first total solar eclipse observed from Venezuela in the last century. The shadow path can be seen in Figure 15. Coincidentally it also passed over Falcón State and occurred on a Thursday in a similar month as it was for 1998. A special expedition from the Cagigal Observatory of Caracas went to a small coastal town called Tucacas (68°18′13.5″ W, 10°47′37.9″ N, 0 m above sea level) to make astronomical, atmospheric and meteorological observations a few days previous to the eclipse and during that day (Ugueto, 1916). The local circumstances for this location as deduced observationally by the expedition were: first contact at 9:55:28.6, second contact at 11:26:48.6, third contact at 11:29:19.8, and fourth contact at 13:00:51.2, all these times being given in local time (UT-4.30 at that time). The totality lasted $\sim$2 min 24 s. The atmospheric conditions for the eclipse day were described as very good although some clouds were present momentarily at 11:15. A variation in temperature of -9.2 °C was noted between 10:05 and 11:25 (local time). For

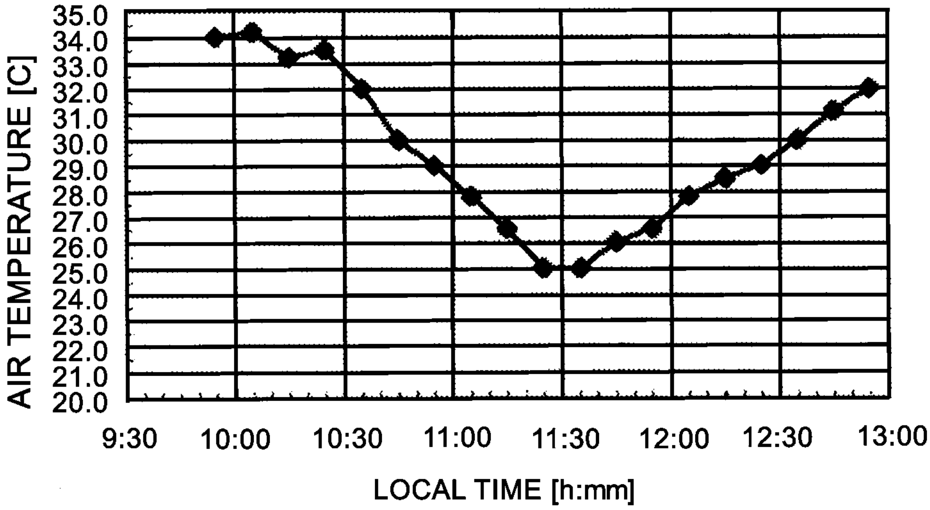

Figure 16. Variation of temperature during the eclipse of 3 February 1916 between 09:55 and 12:55 (local time), measured by the Cagigal Observatory team at Tucacas (Falcón, Venezuela).

Tucacas town Equation (6) and Equation (9) remain the same and Equations (7)–(8) are reduced to,

$$k_{oz} = (0.031/3.0)\{3.0 + 0.4[0.19\cos(\alpha_s) - 0.84]\}, \tag{14}$$

$$k_a = 0.12[1 - (0.32/\ln S)]^{4/3}[1 + 0.33\sin(\alpha_s)], \tag{15}$$

to find, according to Equation (1), the total extinction coefficient in the visual for that particular location during that eclipse. The data for S and t were taken from Ugueto (1916), and the data for α_s was calculated using the software by Duffet-Smith (1997). Figure 16 presents the temperature measurements made the day of this eclipse by the Cagigal Observatory team.

Figure 17 shows the extinction profile for each of the different components contributing to the total extinction as well as the total extinction and relative humidity profiles. It can be seen that, again, the total extinction in the visual is strongly dependent on aerosol extinction ($k_a \gg k_{wv} > k_R > k_{oz}$). During the totality a value of 0.78 mag/air mass for the total global extinction coefficient in the visual was obtained at 11:25, indicating also a poor "night" ($k > 0.5$). In fact, only Venus, Jupiter and Vega (α Lyr), with $m_V = 0.04$ (Allen, 1973), were reported (Ugueto, 1916). In comparing this result with that obtained for the total solar eclipse of 1998 at 14:12 ($k_g \cong 1.11$ mag/air mass), it can be inferred that the eclipse of 1916 was darker than 1998's by a factor of $\sim$0.70; in other words, 30% less bright. This outcome can be appreciated better in terms of visual observations. During the totality of the 1916 eclipse the Cagigal Observatory team could see just one star (Vega) which is less bright than those (Deneb and Fomalhaut) seen by the ARVAL

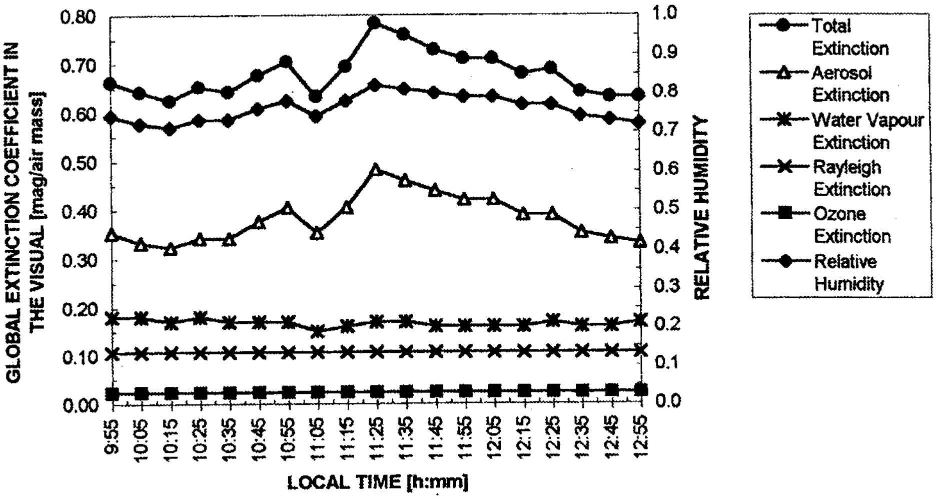

Figure 17. Profile of the global total extinction coefficient in the visual and those for each component contributing to it, during the solar eclipse of 3 February 1916, at Tucacas town (Falcón State, Venezuela) between the first and fourth contacts, calculated from meteorological data provided by Ugueto (1916) and using the same model as in Figure 13. Note again that the total extinction profile is controlled by the aerosol extinction profile. The water vapour profile is also included for comparison purposes.

Observatory team, and Schaefer (1998), respectively, during the totality of the 1998 eclipse. It is surprising, then, that despite its closeness to Vega in the sky, Deneb, being brighter than Vega, was not reported as sighted by the Cagigal team.

Because Tucacas town and Punta de Barco are hot places during the day and throughout the year, the change in temperature during the central phase of the respective eclipses had to be appreciably noted even more for the times when it occurred: the first one at the end of the morning, and the second one near the middle of the afternoon. The first one was "fresher" than the other. In the first one the temperature descended from about 34.2 °C to 25 °C; in the second one from about 30.9 °C to 25.2 °C. Consequently between both eclipses a significant difference of 4.2 °C in the reduction of temperature was found.

It is fair to mention that the Cagigal group also made photometric measurements of the sky during the first part of the eclipse. They used a Heyde aktino photometer which was calibrated with a lamp with only three readings. Subsequently six measurements were made before the second contact, and just one during the totality. The first one, at 09:20 (local time), gave 16.5 instrumental units, and at totality 1.5 instrumental units. Because the units were not specified nor the sky area covered or direction to which their instrument was pointed, a photometric comparison with the 1998 eclipse could not be made. Figure 18 gives a plot of their measurements from which can be seen the reduction of the sky brightness.

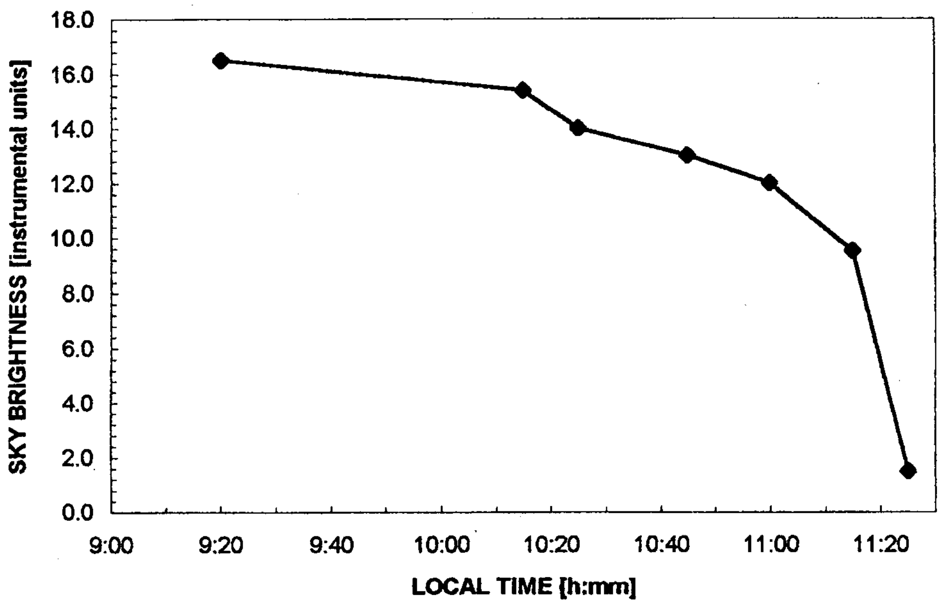

Figure 18. Plot of the photometric measurements made by the Cagigal Observatory group of Caracas, using a Heyde aktino photometer, of the sky brightness during the total solar eclipse of 3 February 1916 at Tucacas town (Falcón State), Venezuela. Because the units were not specified, no comparison could be made.

8. Overview and Conclusions

This paper presents the results of photometric measurements of the intensity of the sky brightness obtained before, during, and after the total solar eclipse of 26 February 1998 at the Caribbean Peninsula of Paraguaná (Falcón State) in Venezuela, in three particular directions: Zenith, horizon anti-parallel or opposite to the umbra path, and horizon perpendicular to this path. These measurements during the totality showed that there was a decrease of three orders of magnitude in the zenith sky brightness as compared to that for noneclipse conditions on that day. Also it was observed that there was a decrease in the horizon sky brightness, perpendicular to the shadow path, by the same order of magnitude as compared with that for the normal day sky in this event. The directions considered on the horizon, and the period of time covered, account for the asymmetry observed in the curves obtained before and after the totality. As a result, consistent with those general obtained for total solar eclipses, the zenith brightness turned out to be less intense than the horizon. In particular, using the sky brightness at full Moon as a reference, the minimum value corresponding to the horizon perpendicular to the shadow path was $\sim$36 times, and that to the zenith was $\sim$14 times brighter, respectively. The zenith brightness during the totality turned out to be 4 times brighter than that measured by James (1998) for the same location. As in previous eclipses, the change in this brightness began to be appreciable when the solar disc was obscured 98.81%.

This paper also presents, in global terms, an estimate of the total extinction coefficient in the visual and their components, produced by Rayleigh scattering, ozone, water vapour and atmospheric aerosol extinction. The results show that atmospheric aerosol is the major component contributing to the total extinction coefficient in the visual, and ozone is a minor one. During the totality this coefficient attained a value of 1.11 mag/air mass which indicates that the darkness produced was indeed very poor. Besides three very bright planets which were clearly seen close to the Sun, only two bright stars were reported to have been sighted at the same time. Therefore, as a first conclusion, the most probable cause explaining this result is the influence of the atmospheric aerosol scattering on the sky brightness during the total phase of the eclipse.

This conclusion is supported by comparisons made with the total solar eclipse of 3 February 1916. The results obtained show that the total global extinction coefficient in the visual is strongly dependent on atmospheric aerosol extinction and less on ozone. During the totality a value of 0.78 mag/air mass was estimated for this coefficient indicating that the darkness produced in that eclipse was also poor. Only one bright star was reported along with three bright planets in the sky of the observation site. Even so, and as a second conclusion, this eclipse was 30% darker than 1998's. Also the temperature variation was greater in the first one than in the second one.

In addition to the above estimates, photometric measurements were used to make estimations of the extinction coefficient (within at least 20% accuracy) before, during, and after the phenomenon for the horizon direction, opposite the shadow path, in the visual. From these estimations a calculation of the mean optical depth in that particular direction was made. The results indicate that the extinction coefficient fluctuated in an irregular manner (between $\sim$0.1–$\sim$1.0 mag/air mass) for the horizon direction. On average a value of $\sim$0.60 mag/air mass was found. The corresponding value for the optical depth was 0.55. An increase of the extinction coefficient during and after the total phase was detected.

It has been photometrically demonstrated that the sky during the totality of the 1998 eclipse was very bright on the horizon as well as at the zenith. This is corroborated by direct visual observations made by this author and by others in the same area which point out that only three planets and only two bright stars could be seen. This general result has in turn been corroborated by applying an empirical model in which astronomical and meteorological data was used. By taking into account the two eclipses considered here, it seems in general terms that, observing phenomena of this type just near the sea, brighter skies are produced during the totality. This conclusion is supported by the results reported by Niranjan and Thulasiraman (1998) of the tropical total solar eclipse of 24 October 1995 for a seaside location on the east coast of India, along with the results reported by Fernández et al. (1983) of the tropical total solar eclipse of 11 July 1991 for some towns along the west coast of Costa Rica on the Pacific Ocean.

It is highly recommended, using future total solar eclipses, to make spectral measurements of the radiance of the eclipsed sky, towards the zenith, in order to attempt additional tests such as those made by Shaw (1978, 1979) of his model (Shaw, 1978). Near the horizon a model explaining the sky colour during a total solar eclipse has been proposed by Gedzelman (1975), which evidently depends on wavelength. In future eclipses of this type an experimental verification of this model is also suggested and expected because so far none has been done.

The central focus of this paper has been first to put emphasis in the influence exerted by atmospheric aerosol on the sky brightness during a tropical total solar eclipse, by using astronomical and meteorological data in an empirical model, and second, along with direct visual reports of stars and planets, to present consistent photometric measurements of this brightness. Nonetheless, based on the work of Darula and Kittler (2000), and Shiozaki et al. (1999), an alternative and interesting approach to study daylight levels at the crucial stages of a solar eclipse has recently been published by Darula et al. (2001) which has been applied by them to the partial solar eclipse of 11 August 1999 over Athens and Bratislava. In the special and extreme case of an eclipsed rising sun, Liu and Zhou (1999) have developed an empirical model to estimate the sky brightness for analysing the curious optical effect known as “double dawn” (Stephenson, 1992; Liu et al., 1999).

Possibly past total solar eclipses were darker (Schove and Fletcher, 1987) than the present ones in populated areas given the anthropogenic alteration of the particle composition of the air today. People at the beginning of the last century, and earlier, could enjoy more this kind of phenomenon from cities and towns. Quoting Ugueto’s historical report of 1916 (in translation from the Spanish): “Through the different phases of the eclipse the book known as “Connaissance des Temps” was set to a distance so that the title on a blue background could be read easily by an observer with normal sight and in broad daylight; the following observations were obtained: At 10^{h} 31^{m} one could read it from 4 metres, at 11^{h} 5^{m} from 3 metres, and during the totality from 0.80 to 1 metre”. From another report (del Castillo et al., 1916) of the observation of the same eclipse in Venezuela, but for a different location (Barquisimeto city; see Figure 15), the following statement was written (in translation from the Spanish): “At the moment of the totality one could read, even though with some little effort. On the *Imitation of Christ*, trans. by Fray Luis de Granada, B. Herder Ed., Friburgh, 1905 [8 point types] one could not read it; and on the *History of the Earth* by L. de Launay, José Ruiz Ed. Madrid, 1907, [12 point types] it could”. Following the division proposed by Silverman and Mullen (1975) it seems that the 1916 eclipse, at Tucacas, can be classified as a light eclipse. A dark eclipse, on the contrary, is that in which print, dials, objects, etc., cannot be distinguished according to this division.

For the 1998 eclipse at Punta de Barco James (1998) reported that small numbers and markings on cameras and lenses, which had been completely invisible during totality from Chile in 1994 (the specific location was not specified), were easily seen at that location; this, in turn, classifies the 1998 eclipse at Punta de Barco as a light eclipse too.

As expected (Meeus, 1982), it will take a long time before another total solar eclipse takes place in Venezuela. Although this will not occur for another 72 years, on 28th September 2071, it is to be hoped that the results presented in this work will contribute to the series of solar eclipse studies in this country started with the pioneering reports on the eclipse of 3 February 1916 and that will keep their continuity in time.

Acknowledgements

First I wish to acknowledge in Venezuela the indispensable financial support provided by the Fundación Polar (Caracas) to cover international and national travel expenses; their co-operation is highly appreciated. Also this acknowledge is extended to Prof. C. Noguera, Faculty of Engineering, Universidad Central (Caracas), and his eclipse team, who provided transport and logistic assistance. Particular thanks are given to Ing°. V. Castro and relatives, wardens of the "Radio Nacional de Venezuela" booster station at Punta de Barco (Paraguaná, Falcón), for his hospitality, friendship, and logistic support. Thanks are also due to Lic. F. Galea of the Biblioteca Central, Universidad Central (Caracas), who kindly provided a copy of the Ugueto's report of 1916 eclipse, and a copy of del Castillo's 1916 eclipse report. I am also indebted to A. Valencia, A. Arnal, and A. Laya of ARVAL Observatory team (Caracas) for providing the meteorological data from their web site, the map of Paraguaná Peninsula presented in this work, and bibliographical assistance. In England, at the University of Essex, I am grateful to Dr. S. Nogues, and Mr. P. Beckwith for their assistance in calibrating the equipment. Mr. T. Trill also gave additional technical support. Mr. T. Vigors and Mr. S. Doubtfire gave very useful computing assistance. Dr. I. Colbeck provided valuable additional financial and administrative support and supplied the equipment used in this work. Also I wish to thank him, along with Mr. M. O'Really, for their collaboration in the revision and correction of the typescript. Dr. D. H. Fremlin and Dr. E. Izquierdo made fruitful mathematical comments. In the United States special thanks are given to Dr. S. Silverman and Dr. J. M. Pasachoff for providing important bibliographical material and scientific information, to Dr. B. Schaefer for his valuable discussion and comments which contributed to improve this paper, and to Dr. F. Espenak for his kindly help in providing eclipse obscuration and other 1998 eclipse calculations. Mr. P. Poitevin helpfully provided a copy of the Sifontes' report from Belgium. Dr. E. Hanna, Dr. B. K. Sapra and Mr. G. Comello supplied relevant references from England, India and The Netherlands, respectively. The University of Los Andes (Mérida-Venezuela), through CELCIEC (Fac. Ciencias), helped to post-edit the figures.

References

Abney, W. de W. and Thorpe: 1889, *Phil. Trans. Roy. Soc. Lond.* **180**, 363.

Allen, C. W.: 1973, *Astrophysical Quantities*, 3rd edn., The Athlone Press, University of London, pp. 176, 239–241.

Anderson, J.: 1999, 'Meteorological Changes during a Solar Eclipse', *Weather* **54**, 207–215.

Baker, D. J.: 1974, 'Rayleigh, the Unit of Light Radiance', *Appl. Opt.* **13**, 2160–2163.

Baker, D. J. and Romick, G. J.: 1976, 'The Rayleigh: Interpretation of the Unit in Terms of Column Emission Rate or Apparent Radiance Expressed in SI Units', *Appl. Opt.* **15**, 1966–1968.

Bansal, M. K. and Verma, T. S.: 1998, 'Aerosol Measurements at Roorkee Relating to the Total Solar Eclipse of 24 Oct. 1995', *Indian J. Radio Space Phys.* **27**, 260–263.

Betenska, N.: 1944, 'Concerning the Brightness of the Sky and the Illumination of the Earth during the Full Phase of a Solar Eclipse', *J. Br. Astron. Assoc.* **54**, 124–125.

Bhattacharyya, J. C.: 1978, *The Eclipse of February 16, 1980 – Path of Totality in India*, Report of India Institute of Astrophysics, Bangalore.

Bose, S., Lal, M., and Ghosh, A. B.: 1997, 'Measurements of Water Vapour over Delhi during the Solar Eclipse – 1995', *Kodaikanal Obs. Bull.* **13**, 183–187.

Brooks, Ch. F., Fergunson, S. P., Kimball, H. H., Haurwitz, B., Brooks, E. S., Namias, J., Pierce, Ch. H., Wexler, H., and Brooks, E. M.: 1941, *Eclipse Meteorology with Special Reference to the Total Solar Eclipse of August 31, 1932*, Harvard Meteorological Studies No. 5, Harvard University (Blue Hill Meteorological Observatory), Milton, MA, 109 pp.

Bruin, F.: 1981, 'Atmospheric Refraction and Extinction near the Horizon', *Arch. Hist. Exact Sci.* **25**, 1–17.

Carman, E. H., Skinner, N. J., and Heeran, M. P.:1981, 'Zenith Sky Brightness and Airglow Emissions during the Equatorial Solar Eclipse of 30 June 1973', *Appl. Opt.* **20**, 778–785.

Dandekar, B. S.: 1968, 'Measurements of the Zenith Sky Brightness and Color during the Total Solar Eclipse of 12 November 1966 at Quehua, Bolivia', *Appl. Opt.* **7**, 705–710.

Dandekar, B. S. and Turtle, J. P.: 1971, 'Day Sky Brightness and Polarization during the Total Solar Eclipse of 7 March 1970', *Appl. Opt.* **10**, 1220–1224.

Dani, K. K. and Devara, P. C. S.: 1996, 'Multispectral Measurements of Aerosol, Optical Thickness around the Total Eclipse of 24 October 1995 over Robertgunj, India', *J. Aerosol Sci.* **27**, S73–S74.

del Castillo, E. A., Freitez, R., Wohnsiedler, S., Torrealba, J. Ma., Fortuna, R., del Castillo, J. M., García, J., de los Santos, F., Briceño, A. S., and Alvarado, R.: 1916, *Our Contribution to the Observations of the Total Solar Eclipse of 3 February 1916*, Tipografía Alvarez. Barquisimeto, Venezuela, 27 pp. (in Spanish).

Darula, S. and Kittler, R.: 2000, 'Daylight during Solar Eclipse', *CTU Rep.* **4**, 29–32.

Darula, S., Kambezides, H. D., and Kittler, R.: 2001, 'Daylight Levels during the Solar Eclipse of 11 August 1999', *Meteorol. Atmos. Phys.* **76**, 251–256.

Duffett-Smith, P.: 1997, *Easy PC Astronomy*, Cambridge University Press, 151 pp.

Espenak, F. and Anderson, J.: 1994, *Total Solar Eclipse of 1995 October 24*, NASA Reference Publication 1344, 73 pp.

Espenak, F. and Anderson, J.: 1996, *Total Solar Eclipse of 1998 February 26*, NASA Reference Publication 1383, 97 pp.

Fernández, W., Castro V., Wright, J., Hidalgo, H., and Sáenz, A.: 1993, 'Changes in Solar Irradiance and Atmospheric Turbidity in Costa Rica during the Total Solar Eclipse of July 11, 1991', *Earth Moon Planets* **63**, 119–132.

Fernández, W., Azofeifa, D. E., and Villalobos, J. A.: 1992, 'El Eclipse Total de Sol del 11 de julio de 1991: Aspectos Generales', in W. Fernández (ed.), *El Eclipse Total de Sol del 11 de Julio de 1991: Observaciones Científicas Realizadas en Costa Rica*, Editorial de la Universidad de Costa Rica, San José.

Fiala, A. D.: 1976, *Solar Eclipses of 1977*, US Naval Observatory Circular No. 156, Washington, D.C., pp. 24–29.

Fiala, A. D. and Lukac, R. L.: 1978, *Total Solar Eclipse of 16 February 1980*, US Naval Observatory Circular No. 158, Washington, D.C.

Gedzelman, S. D.: 1975, 'Sky Color near the Horizon during a Total Solar Eclipse', *Appl. Opt.* **14**, 2831–2837.

González, G.: 1997, 'Ground-Level Humidity, Pressure and Temperature Measurements during the October 24, 1995 Total Solar Eclipse', *Kodaikanal Obs. Bull.* **13**, 151–154.

Halley, E.: 1715, *Phil. Trans. Roy. Soc.* **20**, 145.

Hearnshaw, J. B.: 1992, 'Origins of Stellar Magnitude Scale', *Sky Telesc.* **84**, 494–499.

Hegg, D., Larson, T., and Yuen, P-F.: 1993, 'A Theoretical Study of the Effect of Relative Humidity on Light Scattering by Tropospheric Aerosols', *J. Geophys. Res.* **98D**, 18435–18439.

Hughes, D. W.: 2000, 'Brightness during a Solar Eclipse', *J. Br. Astron. Assoc.* **110**, 203–205.

Hunten, D. M., Roach, F. E., and Chamberlain, J. W.: 1956, 'A Photometric Unit for the Airglow and Aurora', *J. Atmos. Terr. Phys.* **8**, 345–346.

James, N.: 1998, 'The Total Eclipse from Venezuela', *J. Br. Astron. Assoc.* **108**, 127–128.

Jerrard. H. G. and McNeill, D. B.: 1986, *A Dictionary of Scientific Units*, Chapman and Hall, Ltd., 5th edn., London, 117 pp.

Jeske, H.: 1988, 'Meteorology Optics and Radiometeorology', in G. Fischer (ed.), *Landolt-Börnstein Numerical Data and Functional Relationships in Science and Technology*, New Series, V/4b, Springer-Verlag, Berlin, pp. 187–348.

Krisciunas, K. and Schaefer, B. E.: 1991, 'A Model of the Brightness of Moonlight', *Publ. Astron. Soc. Pacific* **102**, 1033–1039.

Kuiper, J. and van der Woude, M.: 1998, 'De Totale Zonsverduistring van 26 Februari 1998(1)', *Meteorologica* **2**, 26–29, (Kuiper, J.) (2) **3**, 32–33, (3) **4**, 21–23.

Lloyd, J. W. F. and Silverman, S. M.: 1971, 'Measurements of the Zenith Sky Intensity and Spectral Distribution during the Solar Eclipse of 12 November 1966 at Bagé, Brazil, and on an Aircraft', *Appl. Opt.* **10**, 1215–1219.

Liu, C-Y. and Zhou, X-L.: 1999, 'The Sky Brightness When the Rising Sun Is in Eclipse', *Chin. Astron. Astrophys.* **23**, 249–257.

Liu, C-Y., Li, J., and Zhou, X-L.: 1999, 'Study on "Double Dawn" ', *Sci. China* (A) **42**, 1224–1232.

Lockyer, W. J. S.: 1927, 'The Degree of Darkness during the Total Solar Eclipse of 1927 June 29', *Mon. Not. R. Astron. Soc.* **88**, 97–101.

Lovell, D. J.: 1953, 'The Concept of Radiation Measurements', *Am. J. Phys.* **21**, 459–452.

Manohar, G. K., Kandalgaonkar, S. S., and Ramana-Murty, Bh. V.: 1985, 'Anomalous Behaviour of Electric Field in the Neighbourhood of Totality of Solar Eclipse', *Indian J. Radio Space Phys.* **14**, 80–81.

Marriott, R. A.: 1999, '1927: A British Eclipse', *J. Br. Astron. Assoc.* **109**, 117–143.

Maske, S. J., Nand, K., Behere P. G., Kachare, S. D., Ghanekar, S. G., and Vaidehi, P.: 1982, 'How Air Pollutant Behaved on the Day of the Solar Eclipse on 16 February 1980', *J. Meteorol. Dept. India* **33**, 133–134.

McCluney, W. R.: 1968, 'Radiometry and Photometry', *Am. J. Phys.* **36**, 977–979.

Meeus, J.: 1982, 'The Frequency of Total and Annular Solar Eclipses for a Given Place', *J. Br. Astron. Assoc.* **92**, 124–126.

Meyer-Arendt, J. R.: 1968, 'Radiometry and Photometry: Units and Conversion Factors', *Appl. Opt.* **7**, 2081–2084.

Middleton, W. E. K.: 1952, *Vision through the Atmosphere*, University of Toronto Press, pp. 6–17.

Miller, R. E. and Fastie, W. G.: 1972, 'Skylight Intensity, Polarization and Airglow Measurements during the Total Solar Eclipse of 30 May 1965', *J. Atmos. Terr. Phys.* **34**, 1541–1546.

Niranjan, K. and Thulasiraman, S.: 1998, 'Aerosol Optical Depth and Size Distribution Changes during the Total Solar Eclipse of 24 October 1995', *Terr. Atmos. Oceanic Sci.* **9**, 255–262.

Peñaloza, M., M.A.: 1975, *A Determination of the Local Circumstances of the Partial Solar Eclipse of 13 December 1974 from Photographic Observations*, University of the Andes, Faculty of Science, Department of Physics, Mérida, Venezuela, Internal Report (in Spanish).

Peñaloza, M., M.A., 1999, 'An Investigation of Aerosol Optical Properties: Atmospheric Implications and Influences', Ph.D. Thesis, University of Essex, Colchester, UK, 365 pp.

Röhl, E.: 1932, 'Partial Eclipse of the Sun of 31 August 1932', *Bol. Soc. Venezolana Ciens*, Nat. No. 10, 393–397 (in Spanish).

Rosenberg, G. V.: 1966, *Twilight: A Study in Atmospheric Optics*, Plenum, New York, 160 pp.

Sapra, B. K., Mayya, Y. S., Sawant, V. D., and Nambi, K. S. V.: 1997a, 'Aerosol Measurements at Trombay Relating to the 1995 Eclipse', *Curr. Sci.* **72**, 321–325.

Sapra, B. K., Sunny, F., Kulkarni, P. B., Mahadevan, T. N., and Pandit, G. G.: 1997b, 'Atmospheric Characteristics at Trombay Relating to the October 1995 Solar Eclipse', *Kodaikanal Obs. Bull.* **13**, 161–166.

Schaefer, B. E.: 1986, 'Atmospheric Extinction Effects on Stellar Alignments', *J. Hist. Astron. Suppl. (Archaeoastron.)* **27**, S32–S42.

Schaefer, B. E.: 1993, 'Astronomy and the Limits of Vision', *Vistas Astron.* **36**, 311–361.

Schaefer, B. E.: 1998, 'To the Visual Limits', *Sky Telesc.* **95**, 57–60.

Schove, D. J. and Fletcher, A.: 1987, *Chronology of Eclipses and Comets – AD 1∼1000*, The Boyde Press, Suffolk, UK, 356 pp.

Sharp, W. E., Lloyd, J. W. F., and Silverman, S. M.: 1966, 'Zenith Skylight Intensity and Color during the Total Solar Eclipse of 20 July 1963', *Appl. Opt.* **5**, 787–792.

Sharp, W. E., Silverman, S. M., and Lloyd, J. W. F.: 1971, 'Summary of Sky Brightness Measurements during Eclipses of the Sun', *Appl. Opt.* **10**, 1207–1210.

Shaw, G. E.: 1975, 'Sky Brightness and Polarization during the 1973 African Eclipse', *Appl. Opt.* **14**, 388–394.

Shaw, G. E.: 1978, 'Sky Radiance during a Total Solar Eclipse: A Theoretical Model', *Appl. Opt.* **17**, 272–276.

Shaw, G. E.: 1979, 'Sky Brightness during the 26 February 1979 Eclipse', *Appl. Opt.* **18**, 2362–2363.

Shiozaki, M., Koga, Y., Nakamura, H., Shimazaki, S., and Kojo, S.: 1999, 'Variations in Daylight during Solar Eclipses', in *Proceedings of the CIE Session*, CIE Publ. No. 133, Vol. 1, 267–271.

Sifontes, E.: 1920, 'Meteorological Variations during an Eclipse – The Annular Eclipse of the Sun of 22 November 1919, Seen in Bolivar City, (Venezuela) SA, as a Partial Eclipse', in *Contributions to the Study of the Tropical Climatology in the South Zone of the Orinoco River*, Part 3, Ciudad Bolivar, Venezuela, pp. 34–36 (in Spanish).

Silverman, S. M. and Mullen, E. G.: 1974, *Sky Brightness during Eclipses: A Compendium from Literature*, AFCRL-TR-74-0363, Special Report No. 180, Hanscom USAFB, Massachusetts, 196 pp.

Silverman, S. M. and Mullen, E. G.: 1975, 'Sky Brightness during Eclipses: A Review', *Appl. Opt.* **14**, 2838–2843.

Singh, A. K., Nivas, S., Kumar, A., Rai, J., and Nigam, M. J.: 1999, 'Variations in Atmospheric Aerosols and Electric Conductivity at Roorkee during the Total Solar Eclipse of October 1995', *Indian J. Radio Space Phys.* **28**, 1–10.

Stenz, L. E.: 1929, 'Radiation solaire à l'opacité atmosphérique pendant l'éclipse du soleil du 29.VI.1927 à Jokkmokk, *Gerlands Beitr. Geophysik.* **XXI**, 270–289.

Stephenson, F. R.: 1992, 'A Re-Investigation of the "Double Dawn" Event Recorded in the Bamboo Annals', *Quart. J. Roy. Astron. Soc.* **33**, 91–98.

Tang, N. I.: 1996, 'Chemical and Size Effects of Hygroscopic Aerosols on Light Scattering Coefficients', *J. Geophys. Res.* **101D**, 19245–19250.

Taylor, B. J., Lucke, P. B., and Laulainen, N. S.: 1977, 'Analyses of Atmospheric Extinction Data Obtained by Astronomers – I. A Time-Trend Analysis of Data with Internal Accidental Errors Obtained at Four Observatories', *Atmos. Environ.* **11**, 1–20.

Ugueto, L.: 1916, *The Total Solar Eclipse of 3 February 1916 in Venezuela*, Ministry of Public Instruction – Cagigal Observatory, Litografía Comercio, Caracas, 42 pp. (in Spanish).

USNO: 1939, *Total Eclipse of the Sun – October 1, 1940* (Supplement to the American Ephemeris, 1940). The US Nautical Almanac Office – US Naval Observatory (USNO), Washington, D.C., 57 pp.

Velasquez, D. A.: 1971, 'Zenith Sky Brightness and Color Change during the Total Solar Eclipse of 12 November 1966 at Santa Inés, Perú', *Appl. Opt.* **10**, 1211–1214.

Young, A. T.: 1990, 'How We Perceive Star Brightness', *Sky Telesc.* **79**, 311–313.

Zirker, J. B.: 1995, *Total Eclipses of the Sun*, Princeton University Press, 134 pp.